

# Tractable Bayesian density regression via logit stick–breaking priors

Tommaso Rigon · Daniele Durante

Received: date / Accepted: date

**Abstract** There is an increasing interest in learning how the distribution of a response variable changes with a set of predictors. Bayesian nonparametric dependent mixture models provide a useful approach to flexibly address this goal. However, many formulations are characterized by difficult interpretation and intractable computational methods. Motivated by these issues, we define a class of predictor–dependent infinite mixture models, which relies on a formal representation of the stick–breaking construction via a continuation–ratio logistic regression, within an exponential family representation. This formulation maintains the same desirable properties of popular predictor–dependent stick-breaking priors, but leverages a recent Pólya-Gamma data augmentation to facilitate tractable inference under a broader variety of routine–use computational methods. These methods include Markov Chain Monte Carlo via Gibbs sampling, Expectation Maximization algorithms, and a variational Bayes routine for scalable inference. The al-

gorithms associated with these methods are tested in a toxicology study.

**Keywords** Continuation–ratio logistic regression · Density regression · Gibbs sampling · Expectation–maximization · Pólya-gamma · Variational Bayes

## 1 Introduction

There is a growing interest in density regression methods which allow the entire distribution of a univariate response variable  $y \in \mathcal{Y}$  to be unknown, and changing with a vector of predictors  $\mathbf{x} \in \mathcal{X}$ . Indeed, the increased flexibility provided by these procedures allows relevant improvements in inference and prediction compared to classical regression frameworks, as seen in several applications (e.g. [Dunson and Park, 2008](#); [Griffin and Steel, 2011](#); [Wade et al., 2014](#); [Gutiérrez et al., 2016](#)).

Within a Bayesian nonparametric framework, there is a wide set of alternative methodologies to provide flexible inference for conditional distributions. Most of these methods represent generalizations of the marginal density estimation problem for  $f(y)$ , which is commonly addressed via Bayesian nonparametric mixture models of the form  $f(y) = \int_{\Theta} K(y; \theta) dP(\theta)$ , where  $K(y; \theta)$  is a known parametric kernel indexed by  $\theta \in \Theta$ , and

---

Tommaso Rigon  
Department of Decision Sciences, Bocconi University  
E-mail: [tommaso.rigon@phd.unibocconi.it](mailto:tommaso.rigon@phd.unibocconi.it)

Daniele Durante  
Department of Decision Sciences, Bocconi University  
E-mail: [daniele.durante@unibocconi.it](mailto:daniele.durante@unibocconi.it)

$P(\boldsymbol{\theta})$  denotes an unknown mixing measure which is assigned a flexible prior  $\Pi$ . Popular choices for  $\Pi$  are the Dirichlet process (Ferguson, 1973), the two-parameter Poisson–Dirichlet process (Pitman and Yor, 1997), and other almost surely discrete random measures having a stick-breaking representation (Ishwaran and James, 2001). This choice leads to the infinite mixture model

$$f(y) = \int_{\boldsymbol{\theta}} K(y; \boldsymbol{\theta}) dP(\boldsymbol{\theta}) = \sum_{h=1}^{+\infty} \pi_h K(y; \boldsymbol{\theta}_h), \quad (1)$$

with  $\pi_h = \nu_h \prod_{l=1}^{h-1} (1 - \nu_l)$ ,  $h = 1, \dots, +\infty$ . In (1), the kernel parameters  $\boldsymbol{\theta}_h$ ,  $h = 1, \dots, +\infty$  are distributed according to a base measure  $P_0$ , whereas the stick-breaking weights  $\nu_h \in (0, 1)$ ,  $h = 1, \dots, +\infty$ , have independent Beta( $a_h, b_h$ ) priors, so that  $\sum_{h=1}^{+\infty} \pi_h = 1$  almost surely. Fixing  $a_h = 1$  and  $b_h = a$  leads to a Dirichlet process mixture model, whereas the two-parameter Poisson–Dirichlet process mixture can be obtained letting  $a_h = 1 - a$  and  $b_h = b + ha$ ,  $0 \leq a < 1$  and  $b > -a$ .

Model (1) has key computational benefits in allowing the implementation of simple Markov Chain Monte Carlo methods for posterior inference (e.g. Escobar and West, 1995; Neal, 2000), and provides a consistent procedure for density estimation (e.g. Ghosal et al., 1999; Tokdar, 2006; Ghosal and Van Der Vaart, 2007). This has motivated different generalizations of (1) to incorporate the conditional density inference problem for  $f(y | \mathbf{x}) = f_{\mathbf{x}}(y)$ , by allowing the unknown random mixing measure  $P_{\mathbf{x}}(\boldsymbol{\theta})$  to change with  $\mathbf{x} \in \mathcal{X}$ , under a dependent stick-breaking characterization (MacEachern, 1999, 2000). Popular representations consider predictor-independent mixing weights  $\pi_h$ , and incorporate changes with  $\mathbf{x} \in \mathcal{X}$  in the atoms  $\boldsymbol{\theta}_h(\mathbf{x})$  (e.g. De Iorio et al., 2004; Gelfand et al., 2005; Caron et al., 2006; De la Cruz-Mesía et al., 2007). Although these constructions have desirable theoretical properties (Barrientos et al., 2012; Pati et al., 2013), as noted in MacEachern (2000) and Griffin and Steel (2006), the predictor-independent assumption for the mixing weights can have limited

flexibility in practice, thus requiring the introduction of many mixture components. This has motivated more general formulations allowing also  $\pi_h(\mathbf{x})$ , to change with the predictors. Relevant examples include the order-based dependent Dirichlet process (Griffin and Steel, 2006), the kernel stick-breaking process (Dunson and Park, 2008), the infinite mixture models with predictor-dependent weights (Antoniano-Villalobos et al., 2014), and more recent representations for Bayesian dynamic inference (Gutiérrez et al., 2016). These formulations provide a broader class of priors for Bayesian density regression, and have desirable theoretical properties (Barrientos et al., 2012; Pati et al., 2013). However their flexibility comes at a computational cost. In particular, the availability of simple algorithms for tractable posterior inference is limited by the specific construction and parameterization of these representations.

The above issues motivate alternative formulations which preserve the theoretical properties, but facilitate tractable posterior computation under a broader variety of standard algorithms in Bayesian inference, thus facilitating a wider implementation of nonparametric density regression. We address this goal via a logit stick-breaking prior (LSBP) which relates each stick-breaking weight  $\nu_h(\mathbf{x}) \in (0, 1)$ , to a function  $\eta_h(\mathbf{x}) \in \mathfrak{R}$  of the covariates, using the logistic link. The proposed statistical model is partially related to the probit stick-breaking prior of Rodriguez and Dunson (2011), which leverages the probit link and provides posterior inference via Markov Chain Monte Carlo (MCMC) algorithms. However, in large-scale applications—when either the number of observations or the dimension of the covariates is large—MCMC via Gibbs sampling could face scalability and mixing issues, thus motivating the development of alternative computational routines. As we will outline in Section 3, the logistic mapping allows simple posterior computation under a broader variety of routine-use algorithms beyond MCMC. These include a tractable

Expectation Maximization (EM) routine for point estimation, and simple variational Bayes (VB) for scalable posterior inference. We shall emphasize that the overarching focus of our contribution is not on developing a novel methodological framework for Bayesian density regression, but on providing alternative representations within this well-established class of models which are characterized by improved interpretability and computational tractability for a wider set of algorithms. To our knowledge this goal remains partially unaddressed, but represents a fundamental condition to facilitate routine implementation of Bayesian density regression by the practitioners.

As discussed in Section 3, there is also a formal connection between the LSBP and the hierarchical mixtures of experts (Jordan and Jacobs, 1994; Bishop and Svensén, 2003), for which VB algorithms are available. Ren et al. (2011) noticed a similar connection in their logistic stick-breaking process. However, their focus is exclusively on clustering of spatio-temporal data, and inference is only available via local VB routines based on the bound of Jaakkola and Jordan (2000). Compared to the approaches mentioned above, our contribution is instead designed for a general class of density regression problems and provides additional algorithms—i.e. Gibbs sampling, EM and a global VB—combining the recent Pólya-Gamma data augmentation for Bayesian logistic regression (Polson et al., 2013), and a continuation-ratio representation (Tutz, 1991) of the LSBP which is described in Section 2. The three routines are empirically compared in Section 4 using a real data toxicology study, previously considered in Dunson and Park (2008). Section 5 provides concluding remarks.

## 2 The logit stick-breaking prior (LSBP)

This section presents a formal construction of the LSBP via a continuation-ratio parameterization of the hierar-

chical mechanism assigning the units to mixture components. As a natural extension of model (1), we consider the general class of predictor-dependent infinite mixture models

$$f_{\mathbf{x}}(y) = \int_{\Theta} K_{\mathbf{x}}(y; \boldsymbol{\theta}) dP_{\mathbf{x}}(\boldsymbol{\theta}) = \sum_{h=1}^{+\infty} \pi_h(\mathbf{x}) K_{\mathbf{x}}(y; \boldsymbol{\theta}_h), \quad (2)$$

where  $\pi_h(\mathbf{x}) = \nu_h(\mathbf{x}) \prod_{l=1}^{h-1} \{1 - \nu_l(\mathbf{x})\}$  are predictor-dependent mixing probabilities having a stick-breaking representation (Sethuraman, 1994), and  $K_{\mathbf{x}}(y; \boldsymbol{\theta})$  is a predictor-dependent kernel function indexed by  $\boldsymbol{\theta}$ .

To provide a constructive representation of the LSBP, let us first consider an equivalent formulation of the predictor-dependent mixture model in (2). In particular, following standard hierarchical representations of mixture models, independent samples  $y_1, \dots, y_n$  from the random variable with density function displayed in (2), can be obtained from

$$\begin{aligned} (y_i | G_i = h, \mathbf{x}_i) &\sim K_{\mathbf{x}_i}(y_i; \boldsymbol{\theta}_h), \\ \text{pr}(G_i = h | \mathbf{x}_i) &= \pi_h(\mathbf{x}_i) = \nu_h(\mathbf{x}_i) \prod_{l=1}^{h-1} \{1 - \nu_l(\mathbf{x}_i)\}, \end{aligned} \quad (3)$$

for every unit  $i = 1, \dots, n$ , where  $\boldsymbol{\theta}_h \sim P_0$  and  $G_i \in \{1, 2, \dots, +\infty\}$  the categorical variable denoting the mixture component associated with unit  $i$ . According to (3), every  $G_i$  has probability mass function  $\text{p}(G_i | \mathbf{x}_i) = \prod_{h=1}^{+\infty} \pi_h(\mathbf{x}_i) \mathbb{1}^{(G_i=h)}$ , with  $\pi_h(\mathbf{x}_i) = \nu_h(\mathbf{x}_i) \prod_{l=1}^{h-1} \{1 - \nu_l(\mathbf{x}_i)\}$  and  $\mathbb{1}(\cdot)$  denoting the indicator function. Thus, re-writing  $\nu_1(\mathbf{x}_i), \dots, \nu_h(\mathbf{x}_i), \dots$  as a function of the mixing probabilities  $\pi_1(\mathbf{x}_i), \dots, \pi_h(\mathbf{x}_i), \dots$  via

$$\nu_h(\mathbf{x}_i) = \frac{\pi_h(\mathbf{x}_i)}{1 - \sum_{l=1}^{h-1} \pi_l(\mathbf{x}_i)} = \frac{\text{pr}(G_i = h | \mathbf{x}_i)}{\text{pr}(G_i > h - 1 | \mathbf{x}_i)}, \quad (4)$$

for each  $h = 1, \dots, +\infty$ , allows each  $\nu_h(\mathbf{x}_i)$  to be easily interpreted as the probability of being allocated to component  $h$ , conditionally on the event of surviving to the previous  $1, \dots, h - 1$  components—i.e.  $\nu_h(\mathbf{x}_i) = \text{pr}(G_i = h | G_i > h - 1, \mathbf{x}_i)$ . This result provides a formal characterization of the stick-breaking construction in (3) as the continuation-ratio parameterization

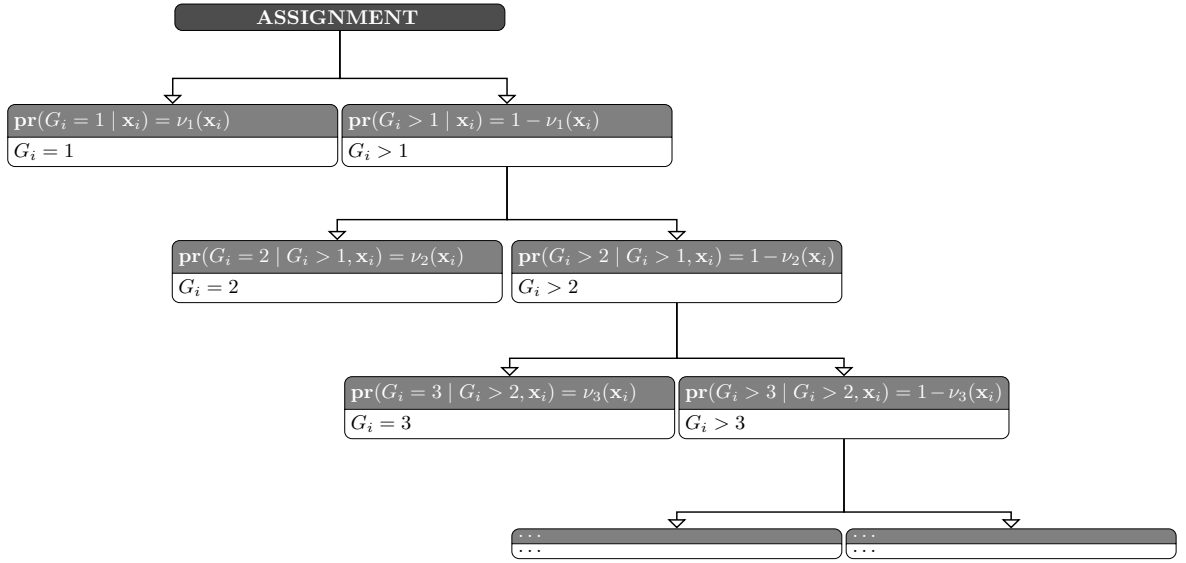


**Fig. 1** Representation of the sequential mechanism to sample  $G_i$ .

(Tutz, 1991) of the probability mass function for each component membership variable  $G_i$ ,  $i = 1, \dots, n$ . This relevant connection with the literature on sequential inference for categorical data is common to all the stick-breaking priors, and provides substantial benefits for interpretation and inference. However, to our knowledge, this characterization—although implicit in some computational routines (e.g. Dunson and Park, 2008; Ren et al., 2011; Rodriguez and Dunson, 2011), and recently adopted in Bayesian multinomial regression (Linderman et al., 2015)—has not yet been explicitly discussed and fully exploited to facilitate interpretation and computation in Bayesian density regression—when  $G_i$ ,  $i = 1, \dots, n$  are latent variables. Indeed, as we describe in Section 3, this characterization facilitates the implementation of different routine-use algorithms in Bayesian inference, and provides a simple generative process for each  $G_i$  which motivates the logistic link.

In particular, according to Figure 1, in the first step of this continuation-ratio generative mechanism, unit  $i$  is either assigned to the first component with probability  $\nu_1(\mathbf{x}_i)$  or to one of the others with complement probability. If  $G_i = 1$  the process stops, otherwise it continues considering the reduced space  $\{2, \dots, +\infty\}$ .

A generic step  $h$  is reached if  $i$  has not been assigned to  $1, \dots, h-1$ , and the decision at this step will be to either allocate  $i$  to component  $h$  with probability  $\nu_h(\mathbf{x}_i)$  or to one of the subsequent components  $h+1, \dots, +\infty$  with probability  $1 - \nu_h(\mathbf{x}_i)$ , conditioned on  $G_i \in \{h, \dots, +\infty\}$ . Based on this representation, each indicator  $\mathbb{1}(G_i = h) = \zeta_{ih}$ ,  $i = 1, \dots, n$ —denoting the assignment to component  $h$ —can be expressed as

$$\zeta_{ih} = z_{ih} \prod_{l=1}^{h-1} (1 - z_{il}), \quad (z_{ih} | \mathbf{x}_i) \sim \text{Bern}\{\nu_h(\mathbf{x}_i)\}, \quad (5)$$

for each  $h = 1, \dots, +\infty$ , where  $z_{ih}$  is a Bernoulli variable denoting the decision at the  $h$ th step to either allocate  $i$  to component  $h$  or to one of the subsequents  $h+1, \dots, +\infty$ . Hence, according to (5), the sampling of each  $G_i$ , under the predictor-dependent stick-breaking representation for each  $\pi_h(\mathbf{x}_i)$  in (3), can be reformulated as a set of sequential Bernoulli choices with natural parameters  $\eta_h(\mathbf{x}_i) = \text{logit}\{\nu_h(\mathbf{x}_i)\} = \log[\nu_h(\mathbf{x}_i)/\{1 - \nu_h(\mathbf{x}_i)\}]$ ,  $h = 1, \dots, +\infty$ , and logistic canonical link, under an exponential family representation. This result motivates the logit stick-breaking factorization

$$\pi_h(\mathbf{x}_i) = \frac{\exp\{\eta_h(\mathbf{x}_i)\}}{1 + \exp\{\eta_h(\mathbf{x}_i)\}} \prod_{l=1}^{h-1} \left[ \frac{1}{1 + \exp\{\eta_l(\mathbf{x}_i)\}} \right], \quad (6)$$

for each  $h = 1, \dots, +\infty$ , while allowing each  $\eta_h(\mathbf{x}_i)$  to be explicitly interpreted as the log-odds of the probability of being allocated to component  $h$  or to one of the subsequents  $h + 1, \dots, +\infty$ , conditionally on the event of surviving to the first  $1, \dots, h - 1$  components. This result facilitates prior specification and posterior inference for the stick-breaking weights, while allowing recent computational advances in Bayesian logistic regression (Polson et al., 2013) to be inherited in our density regression problem.

To conclude our Bayesian representation, we require priors for the log-odds  $\eta_h(\mathbf{x}_i)$  of every  $\nu_h(\mathbf{x}_i)$ , in the continuation–ratio logistic regressions. A natural choice—consistent with classical generalized linear models (e.g. Nelder and Wedderburn, 1972)—is to define  $\eta_h(\mathbf{x}_i)$  as a linear combination of selected functions of the covariates  $\boldsymbol{\psi}(\mathbf{x}_i) = \{\psi_1(\mathbf{x}_i), \dots, \psi_R(\mathbf{x}_i)\}^\top$  and consider Gaussian priors for the coefficients, obtaining

$$\eta_h(\mathbf{x}_i) = \boldsymbol{\psi}(\mathbf{x}_i)^\top \boldsymbol{\alpha}_h, \quad \text{with } \boldsymbol{\alpha}_h \sim N_R(\boldsymbol{\mu}_\alpha, \boldsymbol{\Sigma}_\alpha), \quad (7)$$

for every  $h = 1, \dots, +\infty$ . Although the linearity assumption in (7) may seem restrictive, note that flexible formulations for  $\eta_h(\mathbf{x}_i)$ , including regression via splines and Gaussian processes, induce linear relations in the coefficients. Moreover, as we will outline in Section 3, the linearity assumption simplifies computations, while inducing a logistic-normal prior for each  $\nu_h(\mathbf{x}_i)$ , with well defined moments (Aitchison and Shen, 1980).

Based on the above discussion, the logit stick-breaking does not induce Beta distributed stick-breaking weights, and therefore cannot be included in the general class of stick-breaking priors discussed in Ishwaran and James (2001). However—as discussed in Section 2.1—adapting the theoretical results in Dunson and Park (2008) and Rodriguez and Dunson (2011) to our logistic link, it can be shown that many relevant properties characterizing the priors discussed in Ishwaran and James (2001) are met also under our case. Hence, the LSBP is highly similar in its probabilistic nature and properties to other

popular predictor–dependent stick-breaking constructions (e.g. Dunson and Park, 2008; Rodriguez and Dunson, 2011). However, as discussed in Section 3, differently from the current representations, the LSBP facilitates tractable computations under a broad variety of algorithms for posterior inference.

## 2.1 Properties of the logit stick-breaking prior

Let  $\Theta$  be a complete and separable metric space endowed with the Borel  $\sigma$ -algebra  $\mathcal{B}(\Theta)$ , and let  $\{P_{\mathbf{x}} : \mathbf{x} \in \mathcal{X}\}$  denote the class of predictor–dependent random probability measures on  $\Theta$ , induced by the LSBP

$$P_{\mathbf{x}}(\cdot) = \sum_{h=1}^{+\infty} \pi_h(\mathbf{x}) \delta_{\boldsymbol{\theta}_h}(\cdot), \quad (8)$$

$$\pi_h(\mathbf{x}) = \frac{\exp\{\boldsymbol{\psi}(\mathbf{x}_i)^\top \boldsymbol{\alpha}_h\}}{1 + \exp\{\boldsymbol{\psi}(\mathbf{x}_i)^\top \boldsymbol{\alpha}_h\}} \prod_{l=1}^{h-1} \left[ \frac{1}{1 + \exp\{\boldsymbol{\psi}(\mathbf{x}_i)^\top \boldsymbol{\alpha}_l\}} \right]$$

with independent atoms  $\boldsymbol{\theta}_h \sim P_0$ ,  $h = 1, \dots, +\infty$  from the space  $\{\Theta, \mathcal{B}(\Theta)\}$ , and  $\boldsymbol{\alpha}_h \sim N_R(\boldsymbol{\mu}_\alpha, \boldsymbol{\Sigma}_\alpha)$  independently for every  $h = 1, \dots, +\infty$ . As discussed in Section 2, representation (8) does not provide Beta distributed priors for the logit stick-breaking weights  $\nu_h(\mathbf{x})$ ,  $h = 1, \dots, +\infty$ . However, in line with the random measure outlined in Ishwaran and James (2001), also the LSBP provides a well defined predictor–dependent random probability measure  $P_{\mathbf{x}}$  at every  $\mathbf{x} \in \mathcal{X}$ . This property is formalized in Proposition 1.

**Proposition 1** *For any fixed  $\mathbf{x} \in \mathcal{X}$ ,  $\sum_{h=1}^{+\infty} \pi_h(\mathbf{x}) = 1$  almost surely, with  $\pi_h(\mathbf{x})$  factorized as in (8) and  $\boldsymbol{\alpha}_h \sim N_R(\boldsymbol{\mu}_\alpha, \boldsymbol{\Sigma}_\alpha)$  independently for every  $h = 1, \dots, +\infty$ .*

**Proof:** Recalling results in Ishwaran and James (2001),  $\sum_{h=1}^{+\infty} \pi_h(\mathbf{x}) = 1$  almost surely if and only if the equality  $\sum_{h=1}^{+\infty} \mathbb{E}[\log\{1 - \nu_h(\mathbf{x})\}] = -\infty$  holds. Since  $\log\{1 - \nu_h(\mathbf{x})\}$  is concave in  $\nu_h(\mathbf{x})$  for every  $\mathbf{x} \in \mathcal{X}$  and  $h = 1, \dots, +\infty$ , by the Jensen inequality  $\mathbb{E}[\log\{1 - \nu_h(\mathbf{x})\}] \leq \log[1 - \mathbb{E}\{\nu_h(\mathbf{x})\}]$ . Therefore, since  $\nu_h(\mathbf{x}) \in (0, 1)$ , from the usual properties of the expectation we have that  $0 < \mathbb{E}\{\nu_h(\mathbf{x})\} = \mu_{1\nu}(\mathbf{x}) < 1$ , thereby providing  $\log\{1 -$

$\mu_{1\nu}(\mathbf{x})\} < 0$ . Leveraging these results, the proof of Proposition 1 follows after noticing that  $\sum_{h=1}^{+\infty} \mathbb{E}[\log\{1 - \nu_h(\mathbf{x})\}] \leq \sum_{h=1}^{+\infty} \log\{1 - \mu_{1\nu}(\mathbf{x})\} = -\infty$ .  $\square$

Such property holds also for truncated models based on a finite number of components  $H$ . Indeed, consistent with Ishwaran and James (2001), in this case it suffices to model the first  $H - 1$  weights  $\nu_1(\mathbf{x}), \dots, \nu_{H-1}(\mathbf{x})$  and let  $\nu_H(\mathbf{x}) = 1$  for any  $\mathbf{x} \in \mathcal{X}$ , to ensure  $\sum_{h=1}^H \pi_h(\mathbf{x}) = 1$ .

Results in Proposition 1 motivate further analyses of the logit stick-breaking prior. In particular, consistent with the theoretical studies on other stick-breaking priors not belonging to the class discussed in Ishwaran and James (2001)—e.g. Dunson and Park (2008); Rodriguez and Dunson (2011)—Proposition 2 provides additional insights on the moments of the predictor-dependent random probability measure induced by our logit stick-breaking prior.

**Proposition 2** *For every  $\mathbf{x} \in \mathcal{X}$  and  $B \in \mathcal{B}(\Theta)$  the expectation of  $P_{\mathbf{x}}(B)$  is  $\mathbb{E}\{P_{\mathbf{x}}(B)\} = P_0(B)$ , whereas the variance of  $P_{\mathbf{x}}(B)$  for any truncated version of  $P_{\mathbf{x}}(\cdot)$  in (8) with  $H > 1$ —including the infinite case—is*

$$\text{var}\{P_{\mathbf{x}}(B)\} = P_0(B)\{1 - P_0(B)\} \times \frac{\mu_{2\nu}(\mathbf{x})\{1 - [1 - 2\mu_{1\nu}(\mathbf{x}) + \mu_{2\nu}(\mathbf{x})]^H\}}{2\mu_{1\nu}(\mathbf{x}) - \mu_{2\nu}(\mathbf{x})},$$

where  $\mu_{1\nu}(\mathbf{x}) = \mathbb{E}\{\nu_h(\mathbf{x})\}$  and  $\mu_{2\nu}(\mathbf{x}) = \mathbb{E}\{\nu_h(\mathbf{x})^2\}$  for every  $h = 1, \dots, +\infty$ . The covariance at two different predictor values  $\mathbf{x} \in \mathcal{X}$  and  $\mathbf{x}' \in \mathcal{X}$ ,  $\mathbf{x} \neq \mathbf{x}'$ , is instead

$$\text{cov}\{P_{\mathbf{x}}(B), P_{\mathbf{x}'}(B)\} = P_0(B)\{1 - P_0(B)\} \times \frac{\mu_{2\nu}(\mathbf{x}, \mathbf{x}')\{1 - [1 - \mu_{1\nu}(\mathbf{x}) - \mu_{1\nu}(\mathbf{x}') + \mu_{2\nu}(\mathbf{x}, \mathbf{x}')]^H\}}{\mu_{1\nu}(\mathbf{x}) + \mu_{1\nu}(\mathbf{x}') - \mu_{2\nu}(\mathbf{x}, \mathbf{x}')}$$

with  $\mu_{2\nu}(\mathbf{x}, \mathbf{x}') = \mathbb{E}\{\nu_h(\mathbf{x})\nu_h(\mathbf{x}')\}$ .

**Proof:** Results are a direct consequence of the calculations in Appendix 2 and Appendix 6 in Rodriguez and Dunson (2011), after replacing the probit link with the logistic one.  $\square$

According to Proposition 2, the expectation of  $P_{\mathbf{x}}(\cdot)$  coincides with the base measure  $P_0(\cdot)$  which can be

therefore interpreted as the prior guess for the mixing measure at any  $\mathbf{x} \in \mathcal{X}$ . This quantity is predictor-independent, meaning that a priori we are not forcing particular dependence structure between the atoms  $\theta$  and the predictors. The variance changes instead with the predictors via a function of the first two moments of the logistic-normal stick-breaking weights. Note that, since each  $\nu_h(\mathbf{x})$  is bounded between 0 and 1, we have  $\nu_h(\mathbf{x}) \geq \nu_h(\mathbf{x})^2$  for every  $h = 1, \dots, +\infty$  and  $\mathbf{x} \in \mathcal{X}$ , implying  $0 < \mu_{2\nu}(\mathbf{x}) \leq \mu_{1\nu}(\mathbf{x}) < 1$ . These results provide the bound  $1 - 2\mu_{1\nu}(\mathbf{x}) + \mu_{2\nu}(\mathbf{x}) < 1$ , which leads to a well defined limiting variance for the infinite case  $H \rightarrow +\infty$  equal to  $P_0(B)\{1 - P_0(B)\}\mu_{2\nu}(\mathbf{x})\{2\mu_{1\nu}(\mathbf{x}) - \mu_{2\nu}(\mathbf{x})\}^{-1}$ . The limiting covariance is instead  $P_0(B)\{1 - P_0(B)\}\mu_{2\nu}(\mathbf{x}, \mathbf{x}')\{\mu_{1\nu}(\mathbf{x}) + \mu_{1\nu}(\mathbf{x}') - \mu_{2\nu}(\mathbf{x}, \mathbf{x}')\}^{-1}$ , after noticing that  $\mu_{1\nu}(\mathbf{x}) \geq \mu_{2\nu}(\mathbf{x}, \mathbf{x}')$ ,  $\mu_{1\nu}(\mathbf{x}') \geq \mu_{2\nu}(\mathbf{x}, \mathbf{x}')$  and  $1 - \mu_{1\nu}(\mathbf{x}) - \mu_{1\nu}(\mathbf{x}') + \mu_{2\nu}(\mathbf{x}, \mathbf{x}') < 1$ . Hence the association is always positive and increases the closer  $\mathbf{x}$  is to  $\mathbf{x}'$ .

Although Proposition 2 provides simple expressions for  $\mathbb{E}\{P_{\mathbf{x}}(B)\}$ ,  $\text{var}\{P_{\mathbf{x}}(B)\}$  and  $\text{cov}\{P_{\mathbf{x}}(B), P_{\mathbf{x}'}(B)\}$ , the calculation of these quantities requires the moments of logistic-normal priors for the stick-breaking weights, induced by representation (7). Unfortunately these quantities are not available in explicit form (e.g. Aitchison and Shen, 1980). However, Proposition 3 provides a simple procedure to accurately approximate the moments of logit stick-breaking weights leveraging a connection with the probit stick-breaking priors.

**Proposition 3** *The logit stick-breaking prior described in representation (7), can be accurately approximated by a probit stick-breaking process  $\nu_h(\mathbf{x}) \approx \Phi\{\psi(\mathbf{x})^T \bar{\alpha}_h\}$ , with  $\bar{\alpha}_h = \alpha_h \sqrt{\pi/8} \sim \text{NR}\{\sqrt{\pi/8}\mu_\alpha, (\pi/8)\Sigma_\alpha\}$ , for every  $\mathbf{x} \in \mathcal{X}$  and  $h = 1, \dots, +\infty$ .*

**Proof:** Consistent with results in Amemiya (1981), the logistic link  $\{1 + \exp(-\psi(\mathbf{x})^T \alpha_h)\}^{-1}$  can be accurately

approximated by  $\Phi\{\boldsymbol{\psi}(\mathbf{x})^\top \boldsymbol{\alpha}_h \sqrt{\pi/8}\}$ . Therefore

$$\begin{aligned} \nu_h(\mathbf{x}) &= \{1 + \exp(-\boldsymbol{\psi}(\mathbf{x})^\top \boldsymbol{\alpha}_h)\}^{-1} \approx \Phi\{\boldsymbol{\psi}(\mathbf{x})^\top \boldsymbol{\alpha}_h \sqrt{\pi/8}\} \\ &= \Phi\{\boldsymbol{\psi}(\mathbf{x})^\top \bar{\boldsymbol{\alpha}}_h\}, \end{aligned}$$

with  $\bar{\boldsymbol{\alpha}}_h \sim \sqrt{\pi/8} \mathcal{N}_R(\boldsymbol{\mu}_\alpha, \boldsymbol{\Sigma}_\alpha)$ .  $\square$

According to Proposition 3, the LSBP can be approximated by a PSBP, up to a simple transformation of the prior for the coefficients  $\boldsymbol{\alpha}_h$ . This result allows simple approximation for the moments of the logistic-normal priors on the stick-breaking weights by rescaling those provided in Rodriguez and Dunson (2011) for the PSBP. Moreover, a researcher considering a PSBP, could perform inference leveraging our algorithms, after rescaling the prior for each  $\boldsymbol{\alpha}_h$  by  $\sqrt{8/\pi}$ .

### 3 Bayesian computational methods

Although the LSBP and the associated computational procedures apply to a wider set of dependent mixture models and kernels, we will mainly focus—for the sake of clarity—on the general class of predictor-dependent infinite mixtures of Gaussians

$$\begin{aligned} f_{\mathbf{x}}(y) &= \int \frac{1}{\sigma} \phi\left\{\frac{y - \boldsymbol{\lambda}(\mathbf{x})^\top \boldsymbol{\beta}}{\sigma}\right\} dP_{\mathbf{x}}(\boldsymbol{\beta}, \sigma), \\ &= \sum_{h=1}^{+\infty} \pi_h(\mathbf{x}) \frac{1}{\sigma_h} \phi\left\{\frac{y - \boldsymbol{\lambda}(\mathbf{x})^\top \boldsymbol{\beta}_h}{\sigma_h}\right\}, \end{aligned} \quad (9)$$

with  $\boldsymbol{\beta}_h = (\beta_{1h}, \dots, \beta_{Ph})^\top$  a vector of coefficients linearly related to selected functions of the observed predictors  $\{\lambda_1(\mathbf{x}), \dots, \lambda_P(\mathbf{x})\}^\top$ , comprising the vector  $\boldsymbol{\lambda}(\mathbf{x})$ . Formulation (9) provides a flexible construction (Barrionos et al., 2012; Pati et al., 2013), and is arguably the most used in Bayesian density regression. Generalizations to other kernels will be also discussed.

*Remark 1* Although we focus on density regression via (9), leveraging the prior for the mixing weights induced by (6)–(7), we emphasize that the properties discussed in Section 2, and the algorithms derived in Section

3, hold under more general priors for the predictor-dependent log-odds of the stick-breaking weights. A relevant one can be obtained by replacing (7) with a Gaussian process prior  $\eta_h(\cdot) \sim \text{GP}(0, c_h)$  having squared exponential covariance function  $c_h$ , for  $h = 1, \dots, +\infty$  (e.g. Rasmussen and Williams, 2006). According to Pati et al. (2013), this assumption—combined with model (9)—guarantees full support and posterior consistency as long as the stick-breaking weights are obtained by a monotone differentiable mapping of the Gaussian process prior  $\eta_h(\cdot) \sim \text{GP}(0, c_h)$ . This is the case of the logistic mapping characterizing our LSBP construction.

Besides the above desirable properties, it shall be noticed that under the Gaussian process prior and letting  $\mathbf{x}_1^*, \dots, \mathbf{x}_R^*$  the set of unique values of  $\mathbf{x}_1, \dots, \mathbf{x}_n$ , each  $\eta_h(\mathbf{x}_i)$  can be easily rewritten as in (7), with  $\boldsymbol{\alpha}_h \sim \mathcal{N}_R(\mathbf{0}, \boldsymbol{\Sigma}_\alpha)$ ,  $\boldsymbol{\Sigma}_{\alpha[r r']} = c_h(\mathbf{x}_r^*, \mathbf{x}_{r'}^*)$  and  $\boldsymbol{\psi}(\mathbf{x}_i) = \{\mathbb{1}(\mathbf{x}_i = \mathbf{x}_1^*), \dots, \mathbb{1}(\mathbf{x}_i = \mathbf{x}_R^*)\}^\top$ . This allows the properties discussed in Section 2, and the algorithms in Section 3 to be directly applied to the Gaussian process case.

As mentioned in Section 1, we provide here detailed derivation of three computational methods for Bayesian density regression under model (9), with logit stick-breaking prior (7) for the mixing weights. In particular we consider a Gibbs sampler converging to the exact posterior, an Expectation Maximization (EM) algorithm for fast estimation, and a global variational Bayes (VB) approximation for scalable inference. The algorithms associated with these methods are available at <https://github.com/tommasorigon/LSBP>, along with the code to reproduce the application in Section 4.

All the above computational methodologies exploit representation (3) of model (9)—with  $K_{\mathbf{x}_i}(y_i; \boldsymbol{\theta}_h) = \mathcal{N}(y_i; \boldsymbol{\lambda}(\mathbf{x}_i)^\top \boldsymbol{\beta}_h, \sigma_h^2)$ —and the continuation-ratio characterization of the logit stick-breaking prior in Section 2. In fact, conditioned on the component membership variables  $\mathbf{G} = (G_1, \dots, G_n)$ , the model reduces to a set of Gaussian linear regressions—one for every mix-

ture component—allowing inference for the kernel parameters  $\beta_h$  and  $\sigma_h^2$ , via standard methods when  $\beta_h \sim N_P(\boldsymbol{\mu}_\beta, \boldsymbol{\Sigma}_\beta)$  and  $\sigma_h^{-2} \sim \text{Ga}(a_\sigma, b_\sigma)$ ,  $h = 1, \dots, +\infty$ . Moreover, exploiting  $\mathbf{G}$ , and the continuation–ratio representation, inference for the stick-breaking parameters  $\boldsymbol{\alpha}_h$ ,  $h = 1, \dots, +\infty$  in (7), proceeds as in a Bayesian logistic regression for the data  $(z_{ih} | \mathbf{x}_i) \sim \text{Bern}[\nu_h(\mathbf{x}_i) = \{1 + \exp(-\boldsymbol{\psi}(\mathbf{x}_i)^\top \boldsymbol{\alpha}_h)\}^{-1}]$  in (5), for each  $i = 1, \dots, n$  and  $h = 1, \dots, +\infty$ . Adapting results from the recent Pólya-Gamma data augmentation scheme (Polson et al., 2013) to our statistical model, the updating of  $\boldsymbol{\alpha}_h$ ,  $h = 1, \dots, +\infty$  can be easily accomplished exploiting the following result:

$$\begin{aligned} p_{\mathbf{x}_i}(z_{ih}) &= \frac{0.5 \exp\{(z_{ih} - 0.5)\boldsymbol{\psi}(\mathbf{x}_i)^\top \boldsymbol{\alpha}_h\}}{\cosh\{0.5\boldsymbol{\psi}(\mathbf{x}_i)^\top \boldsymbol{\alpha}_h\}}, \\ f_{\mathbf{x}_i}(\omega_{ih}) &= \frac{\exp[-0.5\{\boldsymbol{\psi}(\mathbf{x}_i)^\top \boldsymbol{\alpha}_h\}^2 \omega_{ih}] f(\omega_{ih})}{[\cosh\{0.5\boldsymbol{\psi}(\mathbf{x}_i)^\top \boldsymbol{\alpha}_h\}]^{-1}}, \end{aligned} \quad (10)$$

independently for every  $i = 1, \dots, n$  and  $h = 1, \dots, +\infty$ , where  $f_{\mathbf{x}_i}(\omega_{ih})$  and  $f(\omega_{ih})$  are the density functions of the Pólya-Gamma random variables  $\text{PG}\{1, \boldsymbol{\psi}(\mathbf{x}_i)^\top \boldsymbol{\alpha}_h\}$ , and  $\text{PG}\{1, 0\}$ , respectively. Hence, based on (10), the contribution to the augmented likelihood for each pair  $(z_{ih}, \omega_{ih})$  is proportional to a Gaussian kernel for transformed data  $(z_{ih} - 0.5)/\omega_{ih}$ , given that  $p_{\mathbf{x}_i}(z_{ih})f_{\mathbf{x}_i}(\omega_{ih}) \propto \exp[(z_{ih} - 0.5)\boldsymbol{\psi}(\mathbf{x}_i)^\top \boldsymbol{\alpha}_h - 0.5\{\boldsymbol{\psi}(\mathbf{x}_i)^\top \boldsymbol{\alpha}_h\}^2 \omega_{ih}]$ . This allows posterior inference under a classical Bayesian linear regression. Refer to Choi and Hobert (2013) for further theoretical properties of the Pólya-Gamma scheme.

Before providing a detailed derivation of the different algorithms available under the LSBP construction, we first study how a truncated version of the random probability measure  $P_{\mathbf{x}}(\boldsymbol{\theta})$  approximates the infinite process. Although there are some computational methods for the infinite representation, these algorithms are not necessarily more tractable than those relying on a finite truncation, and still require approximations. In line with Rodriguez and Dunson (2011) and Ren et al. (2011), we develop detailed routines based on a finite representation, and discuss generalizations to the infi-

nite case. This choice allows more direct comparisons and—based on Theorem 1—provides an accurate approximation of the infinite representation.

**Theorem 1** For a sample  $\mathbf{y} = (y_1, \dots, y_n)^\top$  with covariates  $\mathbf{X} = \{\mathbf{x}_1, \dots, \mathbf{x}_n\}^\top$ , let

$$\begin{aligned} f^{(H)}(\mathbf{y} | \mathbf{X}) &= f_{\mathbf{X}}^{(H)}(\mathbf{y}) = \mathbb{E}_{P_{\mathbf{x}_i}^{(H)}} \left\{ \prod_{i=1}^n f_{\mathbf{x}_i}^{(H)}(y_i) \right\}, \\ &= \mathbb{E}_{P_{\mathbf{x}_i}^{(H)}} \left( \prod_{i=1}^n \left[ \int \frac{1}{\sigma} \phi \left\{ \frac{y_i - \boldsymbol{\lambda}(\mathbf{x}_i)^\top \boldsymbol{\beta}}{\sigma} \right\} dP_{\mathbf{x}_i}^{(H)}(\boldsymbol{\beta}, \sigma) \right] \right), \end{aligned}$$

the marginal joint density of the data based on a truncated version of the LSBP in (6)–(7) with  $H$  components, and let  $f_{\mathbf{X}}^{(\infty)}(\mathbf{y})$  be the same quantity in the infinite case. Then

$$\|f_{\mathbf{X}}^{(H)}(\mathbf{y}) - f_{\mathbf{X}}^{(\infty)}(\mathbf{y})\|_1 \leq 4 \sum_{i=1}^n \{1 - \mu_{1\nu}(\mathbf{x}_i)\}^{H-1}.$$

**Proof:** Adapting the proof of Theorem 1 in Ishwaran and James (2002) to our representation we have that

$$\begin{aligned} \|f_{\mathbf{X}}^{(H)}(\mathbf{y}) - f_{\mathbf{X}}^{(\infty)}(\mathbf{y})\|_1 &\leq 4 \left[ 1 - \mathbb{E} \left\{ \prod_{i=1}^n \sum_{h=1}^{H-1} \pi_h(\mathbf{x}_i) \right\} \right] \\ &= 4\mathbb{E} \left[ 1 - \prod_{i=1}^n \sum_{h=1}^{H-1} \pi_h(\mathbf{x}_i) \right]. \end{aligned}$$

Since  $\sum_{h=1}^{H-1} \pi_h(\mathbf{x}_i) \leq 1$ , and  $1 = \prod_{i=1}^n 1$ , following Lemma 1 in page 358 of Billingsley (1995), we can write  $1 - \prod_{i=1}^n \sum_{h=1}^{H-1} \pi_h(\mathbf{x}_i) = \prod_{i=1}^n [1 - \prod_{h=1}^{H-1} \sum_{h=1}^{H-1} \pi_h(\mathbf{x}_i)] \leq \sum_{i=1}^n \{1 - \sum_{h=1}^{H-1} \pi_h(\mathbf{x}_i)\}$ . This result provides

$$\|f_{\mathbf{X}}^{(H)}(\mathbf{y}) - f_{\mathbf{X}}^{(\infty)}(\mathbf{y})\|_1 \leq 4 \left[ n - \sum_{i=1}^n \sum_{h=1}^{H-1} \mathbb{E}\{\pi_h(\mathbf{x}_i)\} \right],$$

with  $\sum_{h=1}^{H-1} \mathbb{E}\{\pi_h(\mathbf{x}_i)\} = \sum_{h=1}^{H-1} \mu_{1\nu}(\mathbf{x}_i) \{1 - \mu_{1\nu}(\mathbf{x}_i)\}^{H-1} = 1 - \{1 - \mu_{1\nu}(\mathbf{x}_i)\}^{H-1}$ . Substituting this quantity in  $4[n - \sum_{i=1}^n \sum_{h=1}^{H-1} \mathbb{E}\{\pi_h(\mathbf{x}_i)\}]$ , we obtain the final bound  $4 \sum_{i=1}^n \{1 - \mu_{1\nu}(\mathbf{x}_i)\}^{H-1}$ .  $\square$

According to Theorem 1, for fixed  $n$  and  $\mathbf{X}$ , the total variation distance between  $f_{\mathbf{X}}^{(H)}(\mathbf{y})$  and  $f_{\mathbf{X}}^{(\infty)}(\mathbf{y})$  vanishes as  $H \rightarrow +\infty$ , meaning that  $f_{\mathbf{X}}^{(H)}(\mathbf{y})$  converges in distribution to  $f_{\mathbf{X}}^{(\infty)}(\mathbf{y})$  when  $H \rightarrow +\infty$ . This rate of decay is exponential in  $H$ , and therefore the number of components has not to be very large in practice to accurately approximate the infinite representation.



**Algorithm 1:** Steps of the Gibbs sampler for predictor-dependent finite mixtures of Gaussians**begin****[1]** Assign each unit  $i = 1, \dots, n$  to a mixture component  $h = 1, \dots, H$ ;**for**  $i$  from 1 to  $n$  **do**    Sample  $G_i \in (1, \dots, H)$  from the categorical variable with probabilities

$$\text{pr}(G_i = h \mid -) = \frac{\left[ \nu_h(\mathbf{x}_i) \prod_{l=1}^{h-1} \{1 - \nu_l(\mathbf{x}_i)\} \right] \frac{1}{\sigma_h} \phi \left\{ \frac{y_i - \boldsymbol{\lambda}(\mathbf{x}_i)^\top \boldsymbol{\beta}_h}{\sigma_h} \right\}}{\sum_{q=1}^H \left[ \nu_q(\mathbf{x}_i) \prod_{l=1}^{q-1} \{1 - \nu_l(\mathbf{x}_i)\} \right] \frac{1}{\sigma_q} \phi \left\{ \frac{y_i - \boldsymbol{\lambda}(\mathbf{x}_i)^\top \boldsymbol{\beta}_q}{\sigma_q} \right\}},$$

    for every  $h = 1, \dots, H$ .**[2]** Update the parameters  $\boldsymbol{\alpha}_h$ ,  $h = 1, \dots, H - 1$ , for the LSBP, exploiting the continuation-ratio representation and the results from the Pólya-Gamma data augmentation in (10);**for**  $h$  from 1 to  $H - 1$  **do**    **for** every  $i$  such that  $G_i > h - 1$  **do**        Sample the Pólya-Gamma data  $\omega_{ih}$  from  $(\omega_{ih} \mid -) \sim \text{PG}\{1, \boldsymbol{\psi}(\mathbf{x}_i)^\top \boldsymbol{\alpha}_h\}$ .    Given the Pólya-Gamma data, update  $\boldsymbol{\alpha}_h$  from the full conditional  $(\boldsymbol{\alpha}_h \mid -) \sim N_R(\boldsymbol{\mu}_{\boldsymbol{\alpha}_h}, \boldsymbol{\Sigma}_{\boldsymbol{\alpha}_h})$ , having

$$\boldsymbol{\mu}_{\boldsymbol{\alpha}_h} = \boldsymbol{\Sigma}_{\boldsymbol{\alpha}_h} \{ \boldsymbol{\Psi}_h(\mathbf{x})^\top \boldsymbol{\kappa}_h + \boldsymbol{\Sigma}_{\boldsymbol{\alpha}}^{-1} \boldsymbol{\mu}_{\boldsymbol{\alpha}} \}, \boldsymbol{\Sigma}_{\boldsymbol{\alpha}_h} = \{ \boldsymbol{\Psi}_h(\mathbf{x})^\top \boldsymbol{\Omega}_h \boldsymbol{\Psi}_h(\mathbf{x}) + \boldsymbol{\Sigma}_{\boldsymbol{\alpha}}^{-1} \}^{-1}, \boldsymbol{\Omega}_h = \text{diag}(\omega_{i1}, \dots, \omega_{i\bar{n}_h}) \text{ and}$$

$$\boldsymbol{\kappa}_h = (z_{i1} - 0.5, \dots, z_{i\bar{n}_h} - 0.5)^\top, \text{ with } z_{ih} = 1 \text{ if } G_i = h \text{ and } z_{ih} = 0 \text{ if } G_i > h.$$

**[3]** Update the kernel parameters  $\boldsymbol{\beta}_h$ ,  $h = 1, \dots, H$ , in (9), leveraging results from standard Bayesian linear regression;**for**  $h$  from 1 to  $H$  **do**    Sample the coefficients comprising  $\boldsymbol{\beta}_h$  from the full conditional  $(\boldsymbol{\beta}_h \mid -) \sim N_P(\boldsymbol{\mu}_{\boldsymbol{\beta}_h}, \boldsymbol{\Sigma}_{\boldsymbol{\beta}_h})$ , with

$$\boldsymbol{\mu}_{\boldsymbol{\beta}_h} = \boldsymbol{\Sigma}_{\boldsymbol{\beta}_h} \{ \boldsymbol{\Lambda}_h(\mathbf{x})^\top \boldsymbol{\Gamma}_h \mathbf{y}_h + \boldsymbol{\Sigma}_{\boldsymbol{\beta}}^{-1} \boldsymbol{\mu}_{\boldsymbol{\beta}} \}, \boldsymbol{\Sigma}_{\boldsymbol{\beta}_h} = \{ \boldsymbol{\Lambda}_h(\mathbf{x})^\top \boldsymbol{\Gamma}_h \boldsymbol{\Lambda}_h(\mathbf{x}) + \boldsymbol{\Sigma}_{\boldsymbol{\beta}}^{-1} \}^{-1}, \boldsymbol{\Gamma}_h = \sigma_h^{-2} \mathbf{I}_{n_h \times n_h} \text{ and } \mathbf{y}_h \text{ the}$$

$$n_h \times 1 \text{ vector containing the responses for all the units with } G_i = h.$$

**[4]** Update the precision parameters  $\sigma_h^{-2}$ ,  $h = 1, \dots, H$  of each kernel in (9);**for**  $h$  from 1 to  $H$  **do**    Sample  $\sigma_h^{-2}$  from  $(\sigma_h^{-2} \mid -) \sim \text{Ga}[a_\sigma + 0.5 \sum_{i=1}^n \mathbb{1}(G_i = h), b_\sigma + 0.5 \sum_{i:G_i=h} \{y_i - \boldsymbol{\lambda}(\mathbf{x}_i)^\top \boldsymbol{\beta}_h\}^2]$ .

### 3.1 MCMC via Gibbs sampling

In deriving the Gibbs sampling algorithm for the model in (9), with LSBP in (6)–(7), we focus on a dependent mixture of Gaussians with fixed  $H$ . Although we do not derive it in detail here, the generalization to the infinite case is also possible, and can be easily incorporated leveraging the slice samplers of Walker (2007) and Kalli et al. (2011), which introduce a set of augmented latent variables allowing each step of the Gibbs sampler to rely on a finite representation. Such strategy slices the infinite mixture model, reducing it to a finite dimensional problem with  $\bar{H}$  mixture components, where  $\bar{H}$  varies stochastically at each step.

Let  $\boldsymbol{\Lambda}_h(\mathbf{x})$  and  $\boldsymbol{\Psi}_h(\mathbf{x})$  denote the  $n_h \times P$  and the  $\bar{n}_h \times R$  predictor matrices in (9) and (7) having row en-

tries  $\boldsymbol{\lambda}(\mathbf{x}_i)^\top$  and  $\boldsymbol{\psi}(\mathbf{x}_i)^\top$ , for only those statistical units  $i$  such that  $G_i = h$  and  $G_i > h - 1$ , respectively, the Gibbs sampler for the truncated representation of model (9) alternates between the full conjugate updating steps in Algorithm 1. Step [1] can be run in parallel across units  $i = 1, \dots, n$ , whereas parallel computing for the different mixture components  $h = 1, \dots, H$  can be easily implemented in steps [2], [3] and [4].

### 3.2 EM algorithm

In several situations, when either  $P$  or  $n$  are large, the Gibbs sampler described in Section 3.1 could face computational bottlenecks. If a point estimate of model (9) is the main quantity of interest—e.g. for prediction purposes—one possibility in these high-dimensional prob-

---

**Algorithm 2:** Steps of the EM algorithm for predictor–dependent finite mixtures of Gaussians
 

---

**begin**

 Let  $\gamma^{(t)} = (\boldsymbol{\alpha}^{(t)}, \boldsymbol{\beta}^{(t)}, \boldsymbol{\sigma}^{2(t)})$  denote the values of the parameters at iteration  $t$ .

**[1] Expectation:** Exploiting results in (13), the expectation of (12) with respect to the augmented data  $(\zeta_i, \bar{\omega}_i)$ , for each  $i = 1, \dots, n$ , can be simply obtained by plugging in  $\hat{\zeta}_i = \mathbb{E}(\zeta_i | y_i, \mathbf{x}_i, \boldsymbol{\beta}^{(t)}, \boldsymbol{\sigma}^{2(t)})$  and  $\hat{\omega}_i = \mathbb{E}(\bar{\omega}_i | \mathbf{x}_i, \hat{\zeta}_i, \boldsymbol{\alpha}^{(t)})$  in (13). Therefore:

**for**  $i$  from 1 to  $n$  **do**
**for**  $h$  from 1 to  $H$  **do**

 Compute  $\hat{\zeta}_{ih}$  by applying the following expression

$$\hat{\zeta}_{ih} = \frac{\left[ \nu_h^{(t)}(\mathbf{x}_i) \prod_{l=1}^{h-1} \{1 - \nu_l^{(t)}(\mathbf{x}_i)\} \right] \frac{1}{\sigma_h^{(t)}} \phi \left\{ \frac{y_i - \boldsymbol{\lambda}(\mathbf{x}_i)^T \boldsymbol{\beta}_h^{(t)}}{\sigma_h^{(t)}} \right\}}{\sum_{q=1}^H \left[ \nu_q^{(t)}(\mathbf{x}_i) \prod_{l=1}^{q-1} \{1 - \nu_l^{(t)}(\mathbf{x}_i)\} \right] \frac{1}{\sigma_q^{(t)}} \phi \left\{ \frac{y_i - \boldsymbol{\lambda}(\mathbf{x}_i)^T \boldsymbol{\beta}_q^{(t)}}{\sigma_q^{(t)}} \right\}},$$

 and calculate  $\hat{\omega}_{ih}$  via  $\hat{\omega}_{ih} = \{2\psi(\mathbf{x}_i)^T \boldsymbol{\alpha}_h^{(t)}\}^{-1} \tanh \{0.5\psi(\mathbf{x}_i)^T \boldsymbol{\alpha}_h^{(t)}\} \sum_{l=h}^H \hat{\zeta}_{il}$ , (Polson et al., 2013).

**[2] Maximization:** To maximize the expected complete log-posterior  $\log f(\boldsymbol{\alpha}, \boldsymbol{\beta}, \boldsymbol{\sigma}^2 | \mathbf{y}, \hat{\zeta}, \hat{\omega}, \mathbf{x})$ , note that according to (12)–(13), modes  $\boldsymbol{\alpha}^{(t+1)}$  and  $(\boldsymbol{\beta}^{(t+1)}, \boldsymbol{\sigma}^{2(t+1)})$  can be obtained separately as follow:

**for**  $h$  from 1 to  $H - 1$  **do**

 To compute  $\boldsymbol{\alpha}_h^{(t+1)}$ , note that since  $\boldsymbol{\alpha}_h$  has Gaussian prior, and provided that the second term in (13) is based on Gaussian kernels, the estimated  $\boldsymbol{\alpha}_h$  at step  $t + 1$  coincides with the mean of a full conditional Gaussian, similar to the one in step [2] of Algorithm 1.

$$\boldsymbol{\alpha}_h^{(t+1)} = \{\boldsymbol{\Psi}(\mathbf{x})^T \text{diag}(\hat{\omega}_{1h}, \dots, \hat{\omega}_{nh}) \boldsymbol{\Psi}(\mathbf{x}) + \boldsymbol{\Sigma}_{\boldsymbol{\alpha}}^{-1}\}^{-1} \{\boldsymbol{\Psi}(\mathbf{x})^T (\hat{\kappa}_{1h}, \dots, \hat{\kappa}_{nh})^T + \boldsymbol{\Sigma}_{\boldsymbol{\alpha}}^{-1} \boldsymbol{\mu}_{\boldsymbol{\alpha}}\}$$

**for**  $h$  from 1 to  $H$  **do**

A similar approach is can be considered to compute  $\boldsymbol{\beta}_h^{(t+1)}$  and  $\sigma_h^{2(t+1)}$  under the Gaussian and Inverse–Gamma priors for these parameters and the Gaussian kernel characterizing the first term in (13). Hence, adapting steps [3] and [4] in Algorithm 1 to the EM setting, provides:

$$\begin{aligned} \boldsymbol{\beta}_h^{(t+1)} &= \{\boldsymbol{\Lambda}(\mathbf{x})^T \hat{\boldsymbol{\Gamma}}_h^{(t)} \boldsymbol{\Lambda}(\mathbf{x}) + \boldsymbol{\Sigma}_{\boldsymbol{\beta}}^{-1}\}^{-1} \{\boldsymbol{\Lambda}(\mathbf{x})^T \hat{\boldsymbol{\Gamma}}_h^{(t)} \mathbf{y} + \boldsymbol{\Sigma}_{\boldsymbol{\beta}}^{-1} \boldsymbol{\mu}_{\boldsymbol{\beta}}\}, \\ \sigma_h^{-2(t+1)} &= \max\{0, [a_{\sigma} + 0.5 \sum_{i=1}^n \hat{\zeta}_{ih} - 1][b_{\sigma} + 0.5 \sum_{i=1}^n \hat{\zeta}_{ih} \{y_i - \boldsymbol{\lambda}(\mathbf{x}_i)^T \boldsymbol{\beta}_h^{(t)}\}^2]^{-1}\} \\ \text{with } \hat{\boldsymbol{\Gamma}}_h^{(t)} &= \sigma_h^{-2(t)} \text{diag}(\hat{\zeta}_{1h}, \dots, \hat{\zeta}_{nh}). \end{aligned}$$

lems is to rely on a more efficient procedure specifically designed for this goal, such as the EM (Dempster et al., 1977). The implementation of a simple EM for a finite representation of model (9) with LSBP (6)–(7), greatly benefits from the Pólya–Gamma data augmentation, which has analytical expectation and allows direct maximization within a Gaussian linear regression framework. Note that, although the EM algorithm is commonly implemented for maximum likelihood estimation, it can be easily modified to estimate posterior modes (e.g. Dempster et al., 1977).

The EM proposed in Algorithm 2 alternates between a maximization step for the parameters  $(\boldsymbol{\alpha}_h, \boldsymbol{\beta}_h, \sigma_h^2)$ ,  $h = 1, \dots, H$ , and an expectation step for the augmented data  $(\zeta_i, \bar{\omega}_i)$ ,  $i = 1, \dots, n$ , with  $\zeta_i = \{\zeta_{i1} = \mathbb{1}(G_i = 1), \dots, \zeta_{iH} = \mathbb{1}(G_i = H)\}^T$  the vector of binary indicators denoting membership to a mixture component, and  $\bar{\omega}_i = (\bar{\omega}_{i1}, \dots, \bar{\omega}_{iH})^T$  the corresponding Pólya–Gamma augmented data. Note that in this case we work directly with the component indicator variables  $\zeta_i$  instead of the binary vectors  $\mathbf{z}_i = (z_{i1}, \dots, z_{iH})^T$  in (5), to facilitate simpler derivations. Indeed, also un-

der this parameterization, the Pólya-Gamma data augmentation can be easily considered, provided that—according to (3)— $\mathbb{p}(G_i | \mathbf{x}_i)$  can be expressed as

$$\begin{aligned} \mathbb{p}(G_i | \mathbf{x}_i) &= \prod_{h=1}^H \pi_h(\mathbf{x}_i) \mathbb{1}(G_i=h) \\ &= \prod_{h=1}^H \nu_h(\mathbf{x}_i)^{\zeta_{ih}} \{1 - \nu_h(\mathbf{x}_i)\}^{\sum_{l=h}^H \zeta_{il} - \zeta_{ih}}, \end{aligned} \quad (11)$$

for every unit  $i = 1, \dots, n$ . Based on the above quantities, the complete log-posterior  $\log f_{\mathbf{x}}(\boldsymbol{\alpha}, \boldsymbol{\beta}, \boldsymbol{\sigma}^2 | \mathbf{y}, \boldsymbol{\zeta}, \bar{\boldsymbol{\omega}}) = \log f_{\mathbf{x}}(\boldsymbol{\alpha}_1, \dots, \boldsymbol{\alpha}_{H-1}, \boldsymbol{\beta}_1, \dots, \boldsymbol{\beta}_H, \sigma_1^2, \dots, \sigma_H^2 | \mathbf{y}, \boldsymbol{\zeta}, \bar{\boldsymbol{\omega}})$  underlying the proposed EM routine, can be written—up to an additive constant—as

$$\sum_{i=1}^n \ell(\boldsymbol{\alpha}, \boldsymbol{\beta}, \boldsymbol{\sigma}^2; y_i, \boldsymbol{\zeta}_i, \bar{\boldsymbol{\omega}}_i, \mathbf{x}_i) + \log f(\boldsymbol{\alpha})f(\boldsymbol{\beta})f(\boldsymbol{\sigma}^2) \quad (12)$$

where  $\ell(\boldsymbol{\alpha}, \boldsymbol{\beta}, \boldsymbol{\sigma}^2; y_i, \boldsymbol{\zeta}_i, \bar{\boldsymbol{\omega}}_i, \mathbf{x}_i)$  is the contribution of unit  $i$  to the complete log-likelihood, whereas  $f(\boldsymbol{\alpha})$ ,  $f(\boldsymbol{\beta})$ , and  $f(\boldsymbol{\sigma}^2)$  are the prior density functions for the model parameters. Working on  $\ell(\boldsymbol{\alpha}, \boldsymbol{\beta}, \boldsymbol{\sigma}^2; y_i, \boldsymbol{\zeta}_i, \bar{\boldsymbol{\omega}}_i, \mathbf{x}_i)$  has relevant benefits. Indeed, exploiting equations (3) and (11), and the results in Polson et al. (2013), Choi and Hobert (2013) summarized in (10),  $\ell(\boldsymbol{\alpha}, \boldsymbol{\beta}, \boldsymbol{\sigma}^2; y_i, \boldsymbol{\zeta}_i, \bar{\boldsymbol{\omega}}_i, \mathbf{x}_i)$ , can be factorized as  $\ell(\boldsymbol{\beta}, \boldsymbol{\sigma}^2; y_i, \boldsymbol{\zeta}_i, \mathbf{x}_i) + \ell(\boldsymbol{\alpha}; \boldsymbol{\zeta}_i, \bar{\boldsymbol{\omega}}_i, \mathbf{x}_i)$ , where the first summand equals to

$$\sum_{h=1}^H \zeta_{ih} \left[ -\frac{\{y_i - \boldsymbol{\lambda}(\mathbf{x}_i)^{\top} \boldsymbol{\beta}_h\}^2}{2\sigma_h^2} - \frac{1}{2} \log(\sigma_h^2) \right] + \text{const},$$

whereas the second coincides with

$$\sum_{h=1}^{H-1} \bar{\kappa}_{ih} \boldsymbol{\psi}(\mathbf{x}_i)^{\top} \boldsymbol{\alpha}_h + \sum_{h=1}^{H-1} \left[ -\frac{\{\boldsymbol{\psi}(\mathbf{x}_i)^{\top} \boldsymbol{\alpha}_h\}^2}{2\bar{\omega}_{ih}^{-1}} \right] + \text{const},$$

where  $\bar{\kappa}_{ih} = \zeta_{ih} - 0.5 \sum_{l=h}^H \zeta_{il}$ . Hence, the contribution  $\ell(\boldsymbol{\alpha}, \boldsymbol{\beta}, \boldsymbol{\sigma}^2; y_i, \boldsymbol{\zeta}_i, \bar{\boldsymbol{\omega}}_i, \mathbf{x}_i)$  of unit  $i$  to the complete log-likelihood is

$$\begin{aligned} &\sum_{h=1}^H \zeta_{ih} \left[ -\frac{\{y_i - \boldsymbol{\lambda}(\mathbf{x}_i)^{\top} \boldsymbol{\beta}_h\}^2}{2\sigma_h^2} - \frac{1}{2} \log(\sigma_h^2) \right] + \\ &+ \sum_{h=1}^{H-1} \left[ \bar{\kappa}_{ih} \boldsymbol{\psi}(\mathbf{x}_i)^{\top} \boldsymbol{\alpha}_h - \bar{\omega}_{ih} \frac{\{\boldsymbol{\psi}(\mathbf{x}_i)^{\top} \boldsymbol{\alpha}_h\}^2}{2} \right] + \text{const}, \end{aligned} \quad (13)$$

where both terms in equation (13) are linear in the augmented data  $(\boldsymbol{\zeta}_i, \bar{\boldsymbol{\omega}}_i)$ , and represent the sum of Gaussian

kernels. This linearity property simplifies computations in the expectation step for the complete log-posterior in equation (12), whereas the Gaussian structure allows simple maximizations. Since the joint maximization of the expected complete log-posterior with respect to  $(\boldsymbol{\beta}, \boldsymbol{\sigma}^2)$  is intractable, we rely on a conditional maximization procedure in the last step of Algorithm 2, which provides closed form solutions. This approach is referred as Expectation Conditional Maximization (ECM) (Meng and Rubin, 1993).

### 3.3 Mean Field Variational Bayes

Section 3.2 provides a scalable procedure for estimation of posterior modes in large-scale problems. However, an appealing aspect of the Bayesian approach is in allowing uncertainty quantification via inference on the entire posterior distribution. As discussed in Section 3.2, the Gibbs sampler represents an appealing procedure which converges to the exact posterior, but faces computational bottlenecks. This motivates scalable variational methods for approximate and tractable Bayesian inference (Bishop, 2006; Blei et al., 2017).

We seek a variational distribution  $q_{\mathbf{x}}(\boldsymbol{\alpha}, \boldsymbol{\beta}, \boldsymbol{\sigma}^2, \mathbf{z}, \boldsymbol{\omega})$  that best approximates the joint posterior  $f_{\mathbf{x}}(\boldsymbol{\alpha}, \boldsymbol{\beta}, \boldsymbol{\sigma}^2, \mathbf{z}, \boldsymbol{\omega} | \mathbf{y})$ , while maintaining simple computations. This can be obtained by minimizing the Kullback-Leibler divergence  $\text{KL}\{q_{\mathbf{x}}(\boldsymbol{\alpha}, \boldsymbol{\beta}, \boldsymbol{\sigma}^2, \mathbf{z}, \boldsymbol{\omega}) || f_{\mathbf{x}}(\boldsymbol{\alpha}, \boldsymbol{\beta}, \boldsymbol{\sigma}^2, \mathbf{z}, \boldsymbol{\omega} | \mathbf{y})\}$  between the variational distribution and the full posterior, or alternatively by maximizing the evidence lower bound  $\text{ELBO}\{q_{\mathbf{x}}(\boldsymbol{\alpha}, \boldsymbol{\beta}, \boldsymbol{\sigma}^2, \mathbf{z}, \boldsymbol{\omega})\}$  of the log-marginal density  $\log f_{\mathbf{x}}^{(H)}(\mathbf{y})$ , provided that  $\log f_{\mathbf{x}}^{(H)}(\mathbf{y})$  can be analytically expressed as the sum of the ELBO and the positive KL divergence. This lower bound to be maximized, can be expressed as

$$\mathbb{E}_{\boldsymbol{\alpha}, \boldsymbol{\beta}, \boldsymbol{\sigma}^2, \mathbf{z}, \boldsymbol{\omega}} \left[ \log \left\{ \frac{f_{\mathbf{x}}(\mathbf{y}, \boldsymbol{\alpha}, \boldsymbol{\beta}, \boldsymbol{\sigma}^2, \mathbf{z}, \boldsymbol{\omega})}{q_{\mathbf{x}}(\boldsymbol{\alpha}, \boldsymbol{\beta}, \boldsymbol{\sigma}^2, \mathbf{z}, \boldsymbol{\omega})} \right\} \right],$$

where the above expectation is taken with respect to the variational distribution  $q_{\mathbf{x}}(\boldsymbol{\alpha}, \boldsymbol{\beta}, \boldsymbol{\sigma}^2, \mathbf{z}, \boldsymbol{\omega})$ .

**Algorithm 3:** Steps of the VB algorithm for predictor–dependent finite mixtures of Gaussians**begin**Let  $q^{(t)}(\cdot)$  denote the generic variational distribution at iteration  $t$ .**[1]** Compute  $q_{\mathbf{x}_i}^{*(t)}(z_{ih})$ , for each  $i = 1, \dots, n$  and  $h = 1, \dots, H - 1$ ; **for**  $i$  from 1 to  $n$  **do****for**  $h$  from 1 to  $H - 1$  **do**It can be easily shown that the optimal solution for the variational distribution of each  $z_{ih}$  coincides with  $q_{\mathbf{x}_i}^{*(t)}(z_{ih}) = \text{Bern}(\rho_{ih})$ , with

$$\text{logit}(\rho_{ih}) = \boldsymbol{\psi}(\mathbf{x}_i)^\top \mathbf{E}(\boldsymbol{\alpha}_h) + \sum_{l=h}^H \zeta_{il}^{(h)} \left[ 0.5 \cdot \mathbf{E}(\log \sigma_l^{-2}) - 0.5 \cdot \mathbf{E}(\sigma_l^{-2}) \mathbf{E}\{(y_i - \boldsymbol{\lambda}(\mathbf{x}_i)^\top \boldsymbol{\beta}_l)^2\} \right],$$

where the expectations are taken with the respect to the current variational distributions for the other parameters, whereas  $\zeta_{il}^{(h)} = \prod_{r=1}^{l-1} (1 - \rho_{ir})$  if  $l = h$ , and  $\zeta_{il}^{(h)} = -\rho_{il} \prod_{r=1, r \neq h}^{l-1} (1 - \rho_{ir})$  otherwise. Note also that  $\rho_{iH} = 1$ .**[2]** Compute  $q_{\boldsymbol{\alpha}}^{*(t)}(\boldsymbol{\alpha}_h)$ , for each  $h = 1, \dots, H - 1$ ;**for**  $h$  from 1 to  $H - 1$  **do**The optimal solution  $q_{\boldsymbol{\alpha}}^{*(t)}(\boldsymbol{\alpha}_h)$  for the variational distribution of each  $\boldsymbol{\alpha}_h$  is easily available as a Gaussian distribution

$$q_{\boldsymbol{\alpha}}^{*(t)}(\boldsymbol{\alpha}_h) = \text{N}_R[\{\boldsymbol{\Psi}(\mathbf{x})^\top \mathbf{V}_h \boldsymbol{\Psi}(\mathbf{x}) + \boldsymbol{\Sigma}_\alpha^{-1}\}^{-1} \{\boldsymbol{\Psi}(\mathbf{x})^\top \boldsymbol{\rho}_h + \boldsymbol{\Sigma}_\alpha^{-1} \boldsymbol{\mu}_\alpha\}, \{\boldsymbol{\Psi}(\mathbf{x})^\top \mathbf{V}_h \boldsymbol{\Psi}(\mathbf{x}) + \boldsymbol{\Sigma}_\alpha^{-1}\}^{-1}]$$

with  $\mathbf{V}_h = \text{diag}\{\mathbf{E}(\omega_{1h}), \dots, \mathbf{E}(\omega_{nh})\}$  and  $\boldsymbol{\rho}_h = (\rho_{1h} - 0.5, \dots, \rho_{nh} - 0.5)$ .**[3]** Compute the variational distribution  $q_{\mathbf{x}_i}^{*(t)}(\omega_{ih})$  for each  $i = 1, \dots, n$  and  $h = 1, \dots, H - 1$ **for**  $i$  from 1 to  $n$  **do****for**  $h$  from 1 to  $H - 1$  **do**Update the optimal solution  $q_{\mathbf{x}_i}^{*(t)}(\omega_{ih})$ , having Pólya-gamma distribution with parameters

$$q_{\mathbf{x}_i}^{*(t)}(\omega_{ih}) = \text{PG}(1, \xi_{ih}), \quad \xi_{ih}^2 = \boldsymbol{\psi}(\mathbf{x}_i)^\top \mathbf{E}(\boldsymbol{\alpha}_h \boldsymbol{\alpha}_h^\top) \boldsymbol{\psi}(\mathbf{x}_i).$$

From Polson et al. (2013), recall that  $\mathbf{E}(\omega_{ih}) = 0.5 \xi_{ih}^{-1} \tanh(0.5 \xi_{ih})$ , with  $\tanh(\cdot)$  denoting the hyperbolic tangent function.**[4]** Compute  $q_{\boldsymbol{\beta}}^{*(t)}(\boldsymbol{\beta}_h)$  and  $q_{\sigma_h^2}^{*(t)}(\sigma_h^2)$ , for each  $h = 1, \dots, H$ ;**for**  $h$  from 1 to  $H$  **do**Update the optimal solution for the variational distributions of  $\boldsymbol{\beta}_h$  and  $\sigma_h^2$  via

$$q_{\boldsymbol{\beta}}^{*(t)}(\boldsymbol{\beta}_h) = \text{N}_P[\{\boldsymbol{\Lambda}(\mathbf{x})^\top \boldsymbol{\Gamma}_h \boldsymbol{\Lambda}(\mathbf{x}) + \boldsymbol{\Sigma}_\beta^{-1}\}^{-1} \{\boldsymbol{\Lambda}(\mathbf{x})^\top \boldsymbol{\Gamma}_h \mathbf{y} + \boldsymbol{\Sigma}_\beta^{-1} \boldsymbol{\mu}_\beta\}, \{\boldsymbol{\Lambda}(\mathbf{x})^\top \boldsymbol{\Gamma}_h \boldsymbol{\Lambda}(\mathbf{x}) + \boldsymbol{\Sigma}_\beta^{-1}\}^{-1}]$$

$$q_{\sigma_h^2}^{*(t)}(\sigma_h^{-2}) = \text{Ga}[a_\sigma + 0.5 \sum_{i=1}^n \mathbf{E}(\zeta_{ih}), b_\sigma + 0.5 \sum_{i=1}^n \mathbf{E}(\zeta_{ih}) \mathbf{E}\{y_i - \boldsymbol{\lambda}(\mathbf{x}_i)^\top \boldsymbol{\beta}_h\}^2]$$

with  $\boldsymbol{\Gamma}_h = \mathbf{E}(\sigma_h^{-2}) \text{diag}\{\mathbf{E}(\zeta_{1h}), \dots, \mathbf{E}(\zeta_{nh})\}$ .

Without further restrictions, the Kullback-Leibler divergence is minimized when the variational distribution is equal to the true posterior distribution, which is analytically intractable. To address this issue, a common strategy in VB inference (see e.g. Blei et al., 2017) is to assume that the variational distribution belongs to

a mean field variational family. This assumption forces a posteriori independence among distinct groups of parameters, implying that the variational distribution can be expressed as the product of the marginals distributions. Specifically, we let the variational distribution to

factorize in distinct groups

$$q_{\mathbf{x}}(\boldsymbol{\alpha}, \boldsymbol{\beta}, \boldsymbol{\sigma}^2, \mathbf{z}, \boldsymbol{\omega}) = q_{\mathbf{x}}(\boldsymbol{\alpha}, \boldsymbol{\beta}) q_{\mathbf{x}}(\boldsymbol{\sigma}^2) \prod_{h=1}^{H-1} q_{\mathbf{x}}(\mathbf{z}_h, \boldsymbol{\omega}_h), \quad (14)$$

with  $\mathbf{z}_h = (z_{1h}, \dots, z_{nh})$  and  $\boldsymbol{\omega}_h = (\omega_{1h}, \dots, \omega_{nh})$ . Note that we are not making any assumption about the functional form of the distributions  $q_{\mathbf{x}}(\boldsymbol{\alpha}, \boldsymbol{\beta})$ ,  $q_{\mathbf{x}}(\boldsymbol{\sigma}^2)$  and  $\prod_{h=1}^{H-1} q_{\mathbf{x}}(\mathbf{z}_h, \boldsymbol{\omega}_h)$ , neither we are imposing any additional independence structure between the parameters. However, a closer look at the augmented likelihood function  $f_{\mathbf{x}}(\mathbf{y}, \mathbf{z}, \boldsymbol{\omega} \mid \boldsymbol{\alpha}, \boldsymbol{\beta}, \boldsymbol{\sigma}^2) = f_{\mathbf{x}}(\mathbf{y} \mid \mathbf{z}, \boldsymbol{\beta}, \boldsymbol{\sigma}^2) f_{\mathbf{x}}(\mathbf{z} \mid \boldsymbol{\alpha}) f_{\mathbf{x}}(\boldsymbol{\omega} \mid \boldsymbol{\alpha})$ , defined as

$$\prod_{i=1}^n \prod_{h=1}^H \left( \frac{1}{\sigma_h} \phi \left\{ \frac{y_i - \boldsymbol{\lambda}(\mathbf{x}_i)^{\top} \boldsymbol{\beta}_h}{\sigma_h} \right\} \right)^{z_{ih} \prod_{i=1}^{h-1} (1 - z_{ii})} \times \prod_{i=1}^n \prod_{h=1}^{H-1} f(\omega_{ih}) \frac{\exp \{ (z_{ih} - 0.5) \boldsymbol{\psi}(\mathbf{x}_i)^{\top} \boldsymbol{\alpha}_h \}}{\exp \{ 0.5 \omega_{ih} (\boldsymbol{\psi}(\mathbf{x}_i)^{\top} \boldsymbol{\alpha}_h)^2 \}},$$

reveals that the variational distribution in equation (14) can be furtherly factorized exploiting the conditional independence structure between the parameters—which is apparent from the above equation—and independence among prior distributions. This additional simplification is sometimes called induced factorization (Bishop, 2006, Ch. 10.2.5), since it arises from the assumed mean field approximation (14) and the structure of the true posterior distribution. Combining (14) with the factorization induced by the full posterior  $f_{\mathbf{x}}(\boldsymbol{\alpha}, \boldsymbol{\beta}, \boldsymbol{\sigma}^2, \mathbf{z}, \boldsymbol{\omega} \mid \mathbf{y})$ , we obtain

$$q_{\mathbf{x}}(\boldsymbol{\alpha}, \boldsymbol{\beta}, \boldsymbol{\sigma}^2, \mathbf{z}, \boldsymbol{\omega}) = \prod_{h=1}^{H-1} q_{\mathbf{x}}(\boldsymbol{\alpha}_h) \prod_{h=1}^H q_{\mathbf{x}}(\boldsymbol{\beta}_h) \prod_{h=1}^H q_{\mathbf{x}}(\boldsymbol{\sigma}_h^2) \times \prod_{h=1}^{H-1} \prod_{i=1}^n q_{\mathbf{x}_i}(z_{ih}) \prod_{h=1}^{H-1} \prod_{i=1}^n q_{\mathbf{x}_i}(\omega_{ih}).$$

Following Bishop (2006, Ch. 10), the optimal solutions for the variational distribution—under the factorization given in the equation above—have the following form

$$\log q_{\mathbf{x}}^*(\boldsymbol{\beta}_h) = \mathbb{E}_{\boldsymbol{\sigma}^2, \mathbf{z}}[\log \{ f_{\mathbf{x}}(\mathbf{y} \mid \mathbf{z}, \boldsymbol{\beta}, \boldsymbol{\sigma}^2) f(\boldsymbol{\beta}_h) \}] + c_{\boldsymbol{\beta}_h},$$

$$\log q_{\mathbf{x}}^*(\boldsymbol{\sigma}_h^2) = \mathbb{E}_{\boldsymbol{\beta}, \mathbf{z}}[\log \{ f_{\mathbf{x}}(\mathbf{y} \mid \mathbf{z}, \boldsymbol{\beta}, \boldsymbol{\sigma}^2) f(\boldsymbol{\sigma}_h^2) \}] + c_{\boldsymbol{\sigma}_h^2},$$

for every  $h = 1, \dots, H$ , and

$$\log q_{\mathbf{x}_i}^*(z_{ih}) = \mathbb{E}_{\boldsymbol{\alpha}, \boldsymbol{\beta}, \boldsymbol{\sigma}^2, \mathbf{z}_{i,-h}}[\log f_{\mathbf{x}}(\mathbf{y}, \mathbf{z} \mid \boldsymbol{\beta}, \boldsymbol{\sigma}^2 \boldsymbol{\alpha})] + c_{z_{ih}},$$

$$\log q_{\mathbf{x}_i}^*(\omega_{ih}) = \mathbb{E}_{\boldsymbol{\alpha}}[\log f_{\mathbf{x}}(\omega_{ih} \mid \boldsymbol{\alpha})] + c_{\omega_{ih}}, \quad i = 1, \dots, n,$$

$$\log q_{\mathbf{x}}^*(\boldsymbol{\alpha}_h) = \mathbb{E}_{\mathbf{z}, \boldsymbol{\omega}}[\log \{ f_{\mathbf{x}}(\mathbf{z}, \boldsymbol{\omega} \mid \boldsymbol{\alpha}) f(\boldsymbol{\alpha}_h) \}] + c_{\boldsymbol{\alpha}_h},$$

for every  $h = 1, \dots, H - 1$ , where  $\mathbf{z}_{i,-h}$  denotes the vector of binary indicators  $\mathbf{z}_i$  without considering the  $h$ th one, whereas  $c_{\boldsymbol{\beta}_h}$ ,  $c_{\boldsymbol{\sigma}_h^2}$ ,  $c_{\boldsymbol{\alpha}_h}$ ,  $c_{z_{ih}}$  and  $c_{\omega_{ih}}$  are additive constants with respect to the argument in the corresponding variational distribution. Each expectation in the above equations is evaluated with respect to the variational distribution of the other parameters and therefore we need to rely on some iterative method to find the optimal solution. We consider the coordinate ascent variational inference (CAVI) iterative procedure—described in Algorithm 3—which maximizes the variational distribution of each parameter based on the current estimate for the remaining ones (e.g. Bishop, 2006, Ch. 10). This procedure generates a monotonic sequence of the ELBO  $\{q_{\mathbf{x}}(\boldsymbol{\alpha}, \boldsymbol{\beta}, \boldsymbol{\sigma}^2, \mathbf{z}, \boldsymbol{\omega})\}$ , which ensures convergence to a local joint maximum. As shown in Algorithm 3, the normalizing constants in the above equations have not to be computed numerically, since kernels of well known distributions can be recognized.

Finally, we shall emphasize that the novel VB proposed in Algorithm 3 is different from the one in Ren et al. (2011). Indeed—due to the apparent absence of conjugacy for the  $\boldsymbol{\alpha}$  parameters—Ren et al. (2011) rely on a connection with Bayesian hierarchical mixtures of experts (Bishop and Svensén, 2003) and consider the lower bound of Jaakkola and Jordan (2000) to allow simple computation, thus providing a local VB routine (e.g. Bishop, 2006, Ch. 10.5). Leveraging the conjugacy induced by the Pólya-gamma data augmentation, we obtain instead a global mean field VB routine within an exponential family representation. This guarantees that the Kullback-Leibler divergence between the variational distribution and the true posterior is minimized,

and allows recent theoretical properties for this class of computational methods (Blei et al., 2017) to be valid also for our variational algorithm.

#### 4 Epidemiology application

We compare the performance of the three computational methods developed in Section 3, in a toxicology study. Consistent with recent interests in Bayesian density regression (e.g. Dunson and Park, 2008; Hwang and Pennell, 2014; Canale et al., 2017), we focus on a dataset aimed at studying the relationship between the DDE concentration in maternal serum, and the gestational days at delivery (Longnecker et al., 2001).

The DDE is a persistent metabolite of DDT, which is still used against malaria-transmitting mosquitoes in certain developing countries—according to the Malaria Report 2015 from the World Health Organization—thus raising concerns about its adverse effects on premature delivery. Popular studies in reproductive epidemiology address this goal by dichotomizing the gestational age at delivery (GAD) with a clinical threshold, so that births occurred before the 37-th week are considered preterm. Although this approach allows for a simpler modeling strategy, it leads to a clear loss of information. In particular, a greater risk of mortality and morbidity is associated with preterm birth, which increases rapidly as the GAD decreases. This has motivated an increasing interest in modeling how the entire distribution of GAD changes with DDE exposure within a density regression framework (e.g. Dunson and Park, 2008; Hwang and Pennell, 2014; Canale et al., 2017).

As shown in Figure 2, data are composed by  $n = 2,312$  measurements  $(x_i, y_i)$ , for women  $i = 1, \dots, n$ , where  $x_i$  represents the DDE concentration, and  $y_i$  is the gestational age at delivery for woman  $i$ . Our goal is to reproduce the analyses in Dunson and Park (2008) on this dataset, and compare the inference and com-

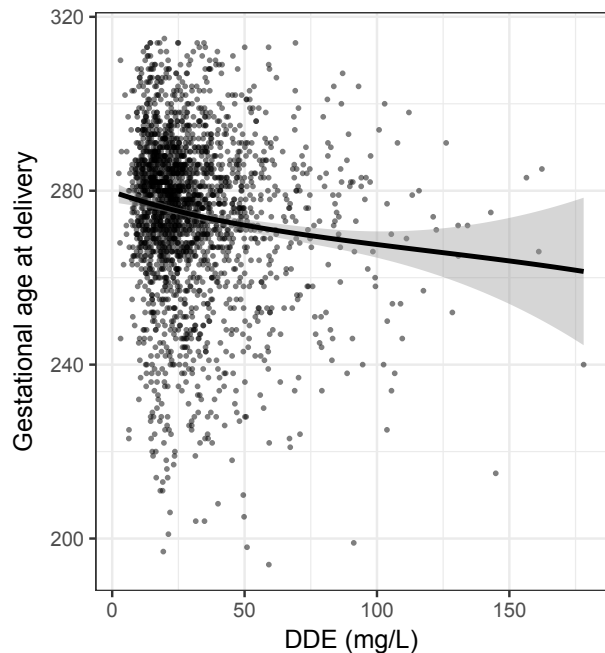


**Fig. 2** Scatterplot of the DDE concentration against the gestational age at delivery, expressed in days, for the 2,312 women in the Longnecker et al. (2001) study. The solid line is a loess estimate for the conditional mean, while the shaded area indicates 95% pointwise confidence intervals.

putational performance of the MCMC via Gibbs sampling, the EM algorithm, and the VB routine proposed in Section 3. Note that, consistent with the main novelty of this contribution, we do not attempt to improve the flexibility and the efficiency of the available statistical models for Bayesian density regression—such as the kernel stick-breaking (Dunson and Park, 2008), and the PSBP (Rodriguez and Dunson, 2011). Indeed, as discussed in Sections 1 and 2, these representations are expected to provide a comparable performance to our LSBP in terms of inference. However, differently from current models for Bayesian density regression, inference under the LSBP is available under a broader variety of computational methods, thus facilitating implementation of the same model in a wider range of applications—including large  $P$  and  $n$  settings. Due to this, the main focus is on providing an empirical comparison of the three algorithms proposed in Section 3,

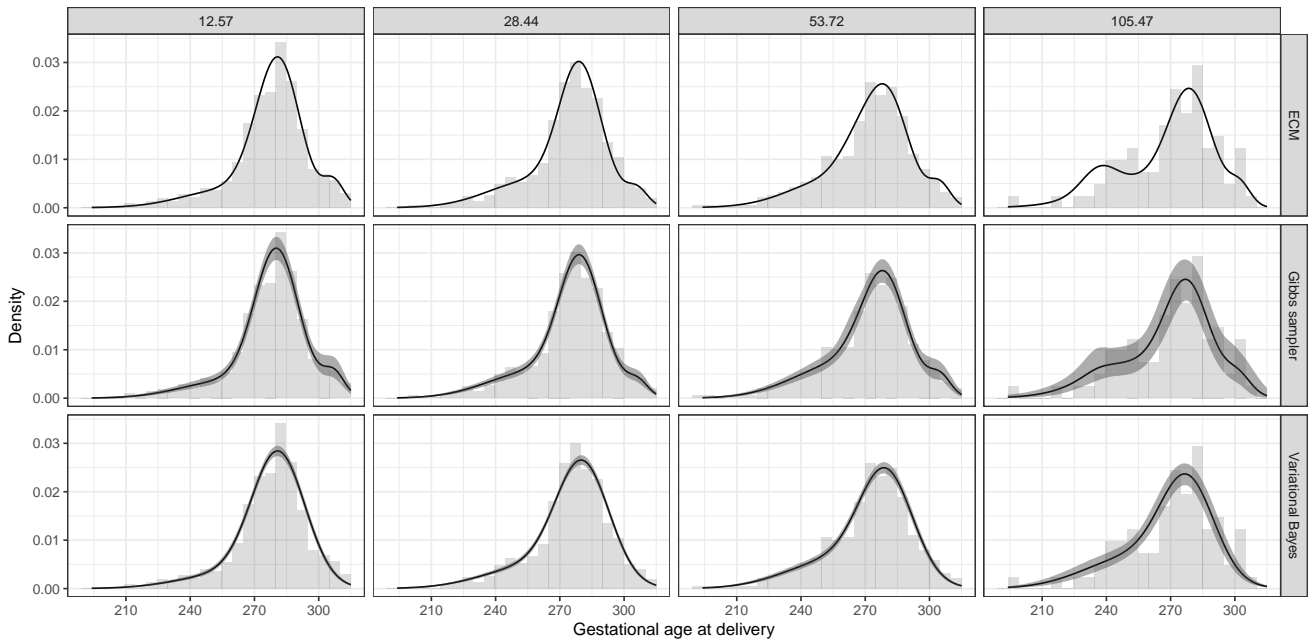


**Fig. 3** For selected quantiles of  $DDE \in (12.57, 28.44, 53.72, 105.47)$ , graphical representation of the posterior mean of the conditional density for  $GAD$  given  $DDE$ , obtained from the Gibbs sampler and the VB, together with 0.95 pointwise credibility intervals (shaded area). Since the EM provides only a mode for the conditional density, we consider a graphical representation of the plug-in estimate for  $f(y | x)$ . The histograms represent the observations of  $GAD$ , having  $DDE$  in the intervals  $(-\infty, 20.505)$ ,  $[20.505, 41.08)$ ,  $[41.08, 79.6)$ ,  $[79.6, +\infty)$ , respectively.

while using results in [Dunson and Park \(2008\)](#) as a benchmark to provide reassurance that inference under the LSBP is comparable to alternative representations widely considered by the practitioners.

We apply the predictor-dependent mixture of Gaussians (9) with LSBP (6)–(7), to a normalized version of the  $DDE$  and  $GAD$   $(\bar{x}_i, \bar{y}_i)$ ,  $i = 1, \dots, n$ , and then show results for  $f_x(y)$  on the original scale of the data. Consistent with previous works ([Dunson and Park, 2008](#); [Canale et al., 2017](#)), we let  $P = 2$ , with  $\lambda_1(\bar{x}_i) = 1$  and  $\lambda_2(\bar{x}_i) = \bar{x}_i$ , for every  $i = 1, \dots, n$ , and rely instead on a flexible representation for  $\eta_h(\bar{x}_i)$  to characterize changes in the stick-breaking weights with  $DDE$ . In particular, each  $\eta_h(\bar{x}_i)$  is defined via a natural cubic spline basis  $\boldsymbol{\psi}(\bar{x}_i) = \{1, \psi_1(\bar{x}_i), \dots, \psi_5(\bar{x}_i)\}^T$ , for every  $h = 1, \dots, H - 1$ . Bayesian posterior inference—under the three computational methods developed in Section 3—is instead performed with default hyperparameters  $\boldsymbol{\mu}_\beta = (0, 0)^T$ ,  $\boldsymbol{\Sigma}_\beta = \mathbf{I}_{2 \times 2}$ ,  $\boldsymbol{\mu}_\alpha = (0, \dots, 0)^T$ ,

$\boldsymbol{\Sigma}_\alpha = \mathbf{I}_{6 \times 6}$  and  $a_\sigma = b_\sigma = 0.1$ . For the total number of mixture components we consider  $H = 5$ , and allow the shrinkage induced by the stick-breaking prior to adaptively delete redundant components not required to characterize the data. As shown in Figure 3, these choices allows accurate inference on  $f_x(y)$ .

In providing posterior inference under the Gibbs sampling algorithm described in Section 3.1, we rely on 30,000 iterations, after discarding the first 5,000 as a burn-in. Analysis of the traceplots for the quantities discussed in Figures 3 and 4 showed that this choice is sufficient for good convergence. The EM algorithm and the VB procedures discussed in Sections 3.2 and 3.3, respectively, are instead run until convergence to a modal solution. Since such modes could be only local, we run both the algorithms for different initial values, and consider the solutions having the highest log-posterior and the lowest bound of the marginal density, respectively. We also controlled the monotonicity of the sequences for

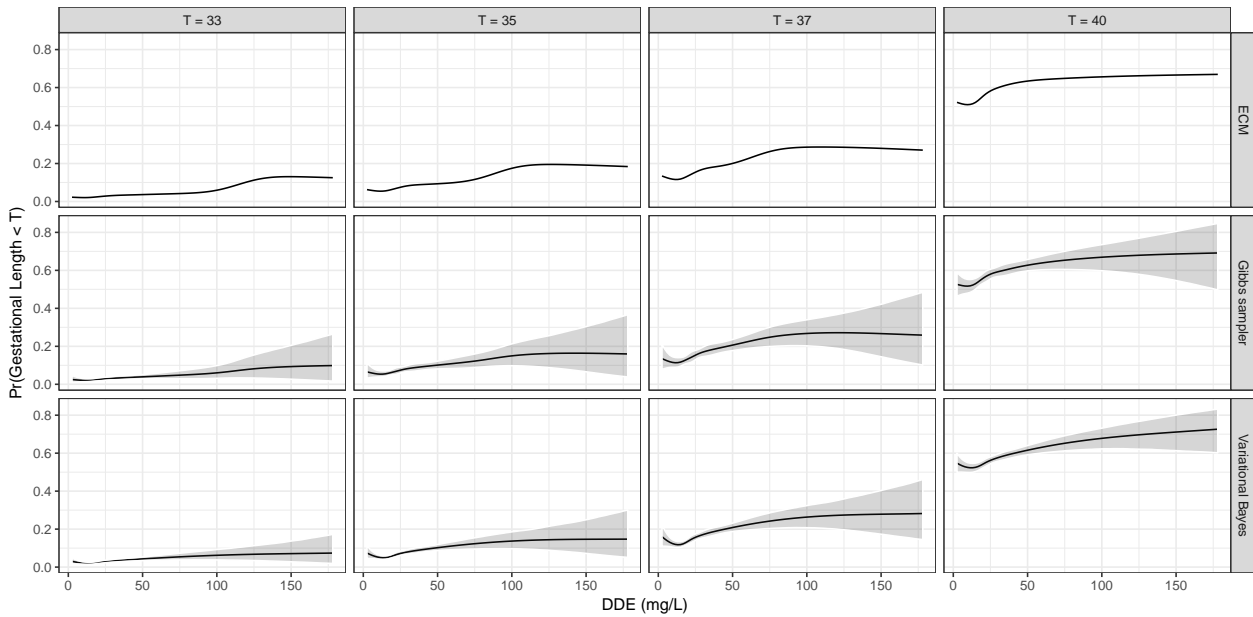


**Fig. 4** For the Gibbs sampler and the VB, posterior means of four different conditional probabilities  $\text{pr}(y < y^* | x)$ —based on thresholds  $y^* \in (7 \cdot 33, 7 \cdot 35, 7 \cdot 37, 7 \cdot 40)$ —along with 0.95 pointwise credibility intervals (shaded area). These quantities are not available from the EM algorithm, for which a plug-in estimate of  $\text{pr}(y < y^* | x)$  is displayed.

these quantities, in order to further validate the correctness of our derivations. In this study, the EM and the VB reach convergence in 2.1 and 6.6 seconds, respectively, whereas the Gibbs sampler requires 5 minutes, using a MacBook Air (OS X Sierra) with a Intel Core i5.

Similarly to Figure 3 in [Dunson and Park \(2008\)](#), Figure 3 provides posterior inference for the conditional density  $f_x(y)$  evaluated at the 0.1, 0.6, 0.9, 0.99 quantiles of DDE, for the three algorithms. Histograms for the GAD, are instead obtained by grouping the response data according to a binning of the DDE with cut-offs at the central values of subsequent quantiles, so that the conditional density can be plotted alongside the corresponding histogram. Results in Figure 3 confirm accurate fit to the data and suggest that the left tail of the GAD distribution—associated with preterm deliveries—increasingly inflates as DDE grows. Moreover, as seen in Figure 3, the three algorithms have similar results, thus providing empirical reassurance for the goodness of the proposed routines. As expected, the point estimate from the EM matches the posterior mean of the Gibbs

sampler, whereas the VB tends to over-smooth some modes of the conditional distribution. This is likely due to the fact that the VB outputs a mean field approximation of the posterior distribution, instead of the exact one. However, differently from the EM, this routine allows uncertainty quantification, and provides a much scalable methodology compared to the Gibbs sampler, thus representing a valid candidate in high-dimensional inference when the focus is on specific functionals of  $f_x(y)$ . Indeed, as shown in Figure 4, when the aim is to exploit  $f_x(y)$  to infer conditional preterm probabilities

$$\text{pr}(y < y^* | x) = \int_{-\infty}^{y^*} f_x(y) dy$$

with  $y^* \in (7 \cdot 33, 7 \cdot 35, 7 \cdot 37, 7 \cdot 40)$  a clinical threshold, the VB provides very similar results compared to the other methods.

Prior to conclude our analysis, note that the results in Figures 3 and 4 are similar to those obtained under the kernel stick-breaking prior in [Dunson and Park \(2008\)](#). This provides empirical guarantee that the flexibility and efficiency properties characterizing popular



Bayesian nonparametric models for density regression are maintained also under our LSBP, which has the additional relevant benefit of facilitating computational implementation of these methodologies. Minor differences are found at extreme DDE exposures, but this is mainly due to the sparsity of the data in this subset of the predictor space, as shown in Figure 2.

## 5 Discussion

The focus of this paper has been on providing novel methodologies to facilitate computational implementation of Bayesian nonparametric models for density regression in a broad range of applications. To address this goal, we have proposed an alternative reparameterization of the predictor-dependent stick-breaking weights, which relies on a set of sequential logistic regressions. This constructive representation has relevant connections with continuation-ratio logistic regressions, and Pólya-Gamma data augmentation, thus allowing simple derivation of several algorithms of routine use in Bayesian inference. The proposed computational methods are empirically evaluated in a toxicology study, obtaining good results and reassurance that the LSBP maintains the same flexibility and efficiency properties characterizing popular Bayesian nonparametric models for density regression.

Although our dependent mixture of Gaussians provides a flexible representation, it is worth considering extensions to other kernels. For example, all our algorithms can be easily adapted to predictor-independent kernels coming from an exponential family, when conjugate priors for their parameters are used. Similar derivations are also possible for predictor-dependent kernels within a generalized linear model representation, provided that conjugate priors for the coefficients can be found (e.g. [Chen and Ibrahim, 2003](#)). Theory and computational steps associated with the logit stick-breaking

prior for the mixing probabilities are instead general and valid regardless the kernel choice.

## References

- Aitchison, J. and S. M. Shen (1980). Logistic-normal distributions: some properties and uses. *Biometrika* 67(2), 262–272. [5](#), [6](#)
- Amemiya, T. (1981). Qualitative response models: a survey. *Journal of Economic Literature* 19(4), 1483–1536. [6](#)
- Antoniano-Villalobos, I., S. Wade, and S. Walker (2014). A Bayesian nonparametric regression model with normalized weights: a study of hippocampal atrophy in Alzheimer’s disease. *Journal of the American Statistical Association* 109(506), 477–490. [2](#)
- Barrientos, A. F., A. Jara, F. A. Quintana, et al. (2012). On the support of maceacherns dependent dirichlet processes and extensions. *Bayesian Analysis* 7(2), 277–310. [2](#), [7](#)
- Billingsley, P. (1995). *Probability and Measure, Third Edition*. Wiley. [8](#)
- Bishop, C. M. (2006). *Pattern Recognition and Machine Learning*. Springer. [11](#), [13](#)
- Bishop, C. M. and M. Svensén (2003). Bayesian hierarchical mixture of experts. In *Proceedings of the Nineteenth Conference of Uncertainty of Artificial Intelligence*. [3](#), [13](#)
- Blei, D. M., A. Kucukelbir, and J. D. McAuliffe (2017). Variational Inference: A Review for Statisticians. *Journal of the American Statistical Association* 112(518), 859–877. [11](#), [12](#), [14](#)
- Canale, A., D. Durante, and D. B. Dunson (2017). Convex mixture regression for quantitative risk assessment. *eprint arXiv:1701.02950*. [14](#), [15](#)
- Caron, F., M. Davy, A. Doucet, E. Duflos, and P. Vanheeghe (2006). Bayesian inference for dynamic models with Dirichlet process mixtures. In *Information*

- Fusion, 2006 9th International Conference on*, pp. 1–8. IEEE. [2](#)
- Chen, M.-H. and J. G. Ibrahim (2003). Conjugate priors for generalized linear models. *Statistica Sinica* *13*, 461–476. [17](#)
- Choi, H. M. and J. P. Hobert (2013). The Poly-Gamma Gibbs sampler for Bayesian logistic regression is uniformly ergodic. *Electronic Journal of Statistics* *7*, 2054–2064. [8](#), [11](#)
- De Iorio, M., P. Müller, G. L. Rosner, and S. N. MacEachern (2004). An ANOVA model for dependent random measures. *Journal of the American Statistical Association* *99*(465), 205–215. [2](#)
- De la Cruz-Mesía, R., F. A. Quintana, and P. Müller (2007). Semiparametric Bayesian classification with longitudinal markers. *Journal of the Royal Statistical Society: Series C (Applied Statistics)* *56*(2), 119–137. [2](#)
- Dempster, A. P., N. M. Laird, and D. B. Rubin (1977). Maximum likelihood from incomplete data via the EM algorithm. *Journal of the Royal Statistical Society, Series B* *39*(1), 1–38. [10](#)
- Dunson, D. B. and J. H. Park (2008). Kernel stick-breaking processes. *Biometrika* *95*(2), 307–323. [1](#), [2](#), [3](#), [4](#), [5](#), [6](#), [14](#), [15](#), [16](#)
- Escobar, M. D. and M. West (1995). Bayesian density estimation and inference using mixtures. *Journal of the American Statistical Association* *90*(430), 577–588. [2](#)
- Ferguson, T. S. (1973). A Bayesian analysis of some nonparametric problems. *The Annals of Statistics* *1*, 209–230. [2](#)
- Gelfand, A. E., A. Kottas, and S. N. MacEachern (2005). Bayesian nonparametric spatial modeling with Dirichlet process mixing. *Journal of the American Statistical Association* *100*(471), 1021–1035. [2](#)
- Ghosal, S., J. K. Ghosh, and R. Ramamoorthi (1999). Posterior consistency of Dirichlet mixtures in density estimation. *The Annals of Statistics* *27*(1), 143–158. [2](#)
- Ghosal, S. and A. Van Der Vaart (2007). Posterior convergence rates of Dirichlet mixtures at smooth densities. *The Annals of Statistics* *35*(2), 697–723. [2](#)
- Griffin, J. E. and M. Steel (2006). Order-based dependent Dirichlet processes. *Journal of the American Statistical Association* *10*, 179–194. [2](#)
- Griffin, J. E. and M. F. Steel (2011). Stick-breaking autoregressive processes. *Journal of Econometrics* *162*(2), 383–396. [1](#)
- Gutiérrez, L., R. H. Mena, and M. Ruggiero (2016). A time dependent Bayesian nonparametric model for air quality analysis. *Computational Statistics & Data Analysis* *95*, 161–175. [1](#), [2](#)
- Hwang, B. S. and M. L. Pennell (2014). Semiparametric bayesian joint modeling of a binary and continuous outcome with applications in toxicological risk assessment. *Statistics in Medicine* *33*(7), 1162–1175. [14](#)
- Ishwaran, H. and L. F. James (2001). Gibbs sampling methods for stick-breaking priors. *Journal of the American Statistical Association* *96*, 161–173. [2](#), [5](#), [6](#)
- Ishwaran, H. and L. F. James (2002). Approximate Dirichlet process computing finite normal mixtures: smoothing and prior information. *Journal of Computational and Graphical Statistics* *11*(3), 508–532. [8](#)
- Jaakkola, T. S. and M. I. Jordan (2000). Bayesian parameter estimation via variational methods. *Statistics and Computing* *10*, 25–37. [3](#), [13](#)
- Jordan, M. I. and R. A. Jacobs (1994). Hierarchical mixture of experts and the EM algorithm. *Neural Computation* *6*, 181–214. [3](#)
- Kalli, M., J. E. Griffin, and S. G. Walker (2011, January). Slice sampling mixture models. *Statistics and Computing* *21*(1), 93–105. [9](#)

- Linderman, S., M. Johnson, and R. P. Adams (2015). Dependent multinomial models made easy: Stick-breaking with the pólya-gamma augmentation. In *Advances in Neural Information Processing Systems*, Volume 28, pp. 3456–3464. [4](#)
- Longnecker, M. P., M. A. Klebanoff, H. Zhou, and J. W. Brock (2001). Association between maternal serum concentration of the ddt metabolite dde and preterm and small-for-gestational-age babies at birth. *Lancet* *358*, 110–114. [14](#)
- MacEachern, S. N. (1999). Dependent nonparametric processes. In *Proceedings of the Bayesian Section*, Alexandria, VA: American Statistical Association, pp. 50–55. [2](#)
- MacEachern, S. N. (2000). Dependent Dirichlet processes. Technical report, Department of Statistics, Ohio State University. [2](#)
- Meng, X.-L. and D. B. Rubin (1993). Maximum likelihood estimation via the ECM algorithm: a general framework. *Biometrika* *80*(2), 267–278. [11](#)
- Neal, R. M. (2000). Markov chain sampling methods for Dirichlet process mixture models. *Journal of Computational and Graphical Statistics* *9*(2), 249–265. [2](#)
- Nelder, J. A. and R. W. M. Wedderburn (1972). Generalized linear models. *Journal of the Royal Statistical Society, Series A* *135*(3), 370 – 384. [5](#)
- Pati, D., D. B. Dunson, and S. T. Tokdar (2013). Posterior consistency in conditional distribution estimation. *Journal of Multivariate Analysis* *116*, 456–472. [2, 7](#)
- Pitman, J. and M. Yor (1997). The two-parameter Poisson-Dirichlet distribution derived from a stable subordinator. *The Annals of Probability* *25*(2), 855–900. [2](#)
- Polson, N. G., J. G. Scott, and J. Windle (2013). Bayesian inference for logistic models using Pólya-Gamma latent variables. *Journal of the American Statistical Association* *108*(504), 1339–1349. [3, 5, 8, 10, 11, 12](#)
- Rasmussen, C. and C. Williams (2006). *Gaussian Processes for Machine Learning*. The MIT Press. [7](#)
- Ren, L., L. Du, L. Carin, and D. B. Dunson (2011). Logistic stick-breaking process. *Journal of Machine Learning Research* *12*, 203–239. [3, 4, 8, 13](#)
- Rodriguez, A. and D. B. Dunson (2011). Nonparametric Bayesian models through probit stick-breaking processes. *Bayesian Analysis* *6*(1), 145–178. [2, 4, 5, 6, 7, 8, 14](#)
- Sethuraman, J. (1994). A constructive definition of Dirichlet priors. *Statistica Sinica* *4*, 639–650. [3](#)
- Tokdar, S. T. (2006). Posterior consistency of dirichlet location-scale mixture of normals in density estimation and regression. *Sankhyā: The Indian Journal of Statistics*, 90–110. [2](#)
- Tutz, G. (1991). Sequential models in categorical regression. *Computational Statistics & Data Analysis* *11*, 275–295. [3, 4](#)
- Wade, S., D. B. Dunson, S. Petrone, and L. Trippa (2014). Improving Prediction from Dirichlet Process Mixtures via Enrichment. *Journal of Machine Learning Research* *15*, 1041–1071. [1](#)
- Walker, S. G. (2007). Sampling the Dirichlet mixture model with slices. *Communications in Statistics – Simulation and Computation* *36*, 45–54. [9](#)